Title: The Lactate Receptor GPR81 is a Mechanism of Leukemia-Associated Macrophage Polarization in the Bone Marrow Microenvironment

Authors and Affiliations: Celia A. Soto[1,2,3], Maggie L. Lesch[2,4], Jennifer L. Becker[5], Azmeer Sharipol[2,3,6], Amal Khan[2,3,4], Xenia L. Schafer[7], Michael W. Becker[2,8], Joshua C. Munger[4,7], Benjamin J. Frisch[1,2,3,6]

[1]Department of Pathology and Laboratory Medicine, University of Rochester School of Medicine, Rochester, NY, USA

[2]Wilmot Cancer Institute, University of Rochester Medical Center, Rochester, NY, USA

[3]Center for Musculoskeletal Research, University of Rochester Medical Center, Rochester, NY, USA

[4]Department of Microbiology and Immunology, University of Rochester School of Medicine, Rochester, NY, USA

[5]Genomics Research Center, University of Rochester Medical Center, Rochester, NY, USA

[6]Department of Biomedical Engineering, University of Rochester School of Medicine, Rochester, NY, USA

[7]Department of Biochemistry and Biophysics, University of Rochester School of Medicine, Rochester, NY, USA

[8]Department of Medicine, University of Rochester School of Medicine, Rochester, NY, USA

Running Head: Lactate-GPR81 Signaling in Leukemia-Associated Macrophages

Keywords: Acute myeloid leukemia (AML), bone marrow microenvironment, GPR81, lactate, macrophages

Corresponding Author: Benjamin J. Frisch, Ph.D., University of Rochester Medical Center, School of Medicine and Dentistry. 601 Elmwood Avenue, Box 704, Rochester, NY, 14642. 1-(585)-275-5082, Benjamin_Frisch2@urmc.rochester.edu

Competing Interests: Authors have no competing interest to declare.

Total Number of Figures and Tables: 6 main figures, 6 supplementary figures, 4 tables, 5 supplementary tables, and 2 supplementary methods tables.

Abstract

Interactions between acute myeloid leukemia (AML) and the bone marrow microenvironment (BMME) are critical to leukemia progression and chemoresistance. Altered metabolite levels in the tumor microenvironment contribute to immunosuppression in solid tumors, while this has not been studied yet in the leukemic BMME. Metabolomics of AML patient bone marrow serum detected elevated metabolites, including lactate, compared to age- and sex-matched controls. Excess lactate has been implicated in solid tumors for inducing suppressive tumor-associated macrophages (TAMs) and correlates with poor prognosis. We describe the role of lactate in the polarization of leukemia-associated macrophages (LAMs) using a murine model of blast crisis chronic myelogenous leukemia (bcCML) and mice genetically lacking the lactate receptor GPR81. LAMs were CD206^{hi} and suppressive in transcriptomics and cytokine profiling. Yet, LAMs had a largely unique expression profile from other types of TAMs. We demonstrate GPR81 signaling as a mechanism of both LAM polarization and the direct support of leukemia cell growth and self-repopulation. Furthermore, LAMs and elevated lactate diminished the function of hematopoietic progenitors and stromal support, while knockout of GPR81 had modest protective effects on the hematopoietic system. We report microenvironmental lactate as a critical driver of AML-induced immunosuppression and leukemic progression, thus identifying GPR81 signaling as an exciting and novel therapeutic target for treating this devastating disease.

INTRODUCTION

Acute myeloid leukemia (AML) is within the top ten cancer subtypes that have the greatest number of deaths per year in the U.S. [SEER, NIH]. It has a nearly 90% mortality rate at five years past diagnosis in the most affected age group of greater than 65 years of age (1). Myeloid cells are an important class of blood and immune cells, including macrophages, neutrophils, megakaryocytes, and erythrocytes. AML is a hematologic malignancy initiated by genetic mutations in immature myeloid progenitor cells. Leukemic blasts undergo an uncontrolled proliferation (clonal hematopoiesis) and then accumulate in the bone marrow (BM) and other tissues (2). Dysfunction of the bone marrow microenvironment (BMME) ensues, leading to a loss of normal blood cell production and an immune-suppressed BM. These are critical factors in fatality due to infection, hemorrhage, or BM failure (3,4). Chemotherapies initially reduce leukemic burden; however, relapse occurs in most patients, and there are various adverse effects on already stressed hematopoietic tissues (5,6). With approximately 20,000 new cases annually in the United States alone [SEER, NIH] and an increasing global incidence (7), there is a clear, unmet need for novel treatment options.

Immunotherapy has been an avenue of recent innovation in treating cancer, yet implementing effective and safe immunotherapies for AML remains challenging. The development of immunotherapy that will specifically target myeloid leukemia cells is especially difficult because tumor specific antigens are also found on noncancerous myeloid cells. Furthermore, thus far, the combination of chemotherapy and immunotherapy has not yet been effective in clearing leukemic stem cell (LSC) populations that lead to relapse in AML (8). In addition, the therapeutic triggering of an immune response in the BM to kill leukemia cells must be carried out with care not to harm the important blood progenitor cells that are produced there. Still, immunotherapies have been greatly successful in the treatment of other types of leukemia; there are currently ten FDA-approved immunotherapies for lymphoblastic leukemias, such as CAR T cell therapies and targeted antibodies. This warrants further investigation for myeloid leukemia immunotherapy.

Signaling within the BMME directs all blood cell precursors to be produced from hematopoietic stem cells (HSCs). When not circulating, HSCs reside at endosteal and perivascular areas within the BM, termed HSC “niches”, where they receive signals from specialized cells to remain quiescent, self-renew, or exit the niche to begin to differentiate into hematopoietic progenitors. Multiple cell types have been implicated in the regulation of HSCs including specialized subsets of mesenchymal stromal cells (MSCs) (9,10), osteoblasts (OBs) (11,12), endothelial cells (13-15), and macrophages (16). Niche cells signal by cell-cell contact and secretion of numerous regulatory factors, including extracellular cytokines and inflammatory molecules (9,17-21). Therefore, the BMME must maintain cellular and extracellular composition for hematopoietic homeostasis. BMME alterations can initiate or support leukemogenesis, and, reciprocally, leukemia results in an altered BMME (22-24). Furthermore, AML cells take refuge at the niche, leading to relapse when LSC populations survive and repopulate after treatment (25,26). A thorough understanding of the microenvironment is needed to improve treatment and identify potentially safe therapeutic targets.

Solid tumor microenvironments have altered levels of extracellular metabolites, which render immune cells ineffective while supporting cancer cells (27,28). Thus far, the contribution of extracellular metabolites to AML progression has not been well-defined. Elevated tumor metabolites are attributed to the amplified metabolic drive of cancer cells and increased cellular density within the tumor (29). In contrast, the BMME has a less compact tumor architecture, with ample vessel availability for nutrient and oxygen transfer throughout. Our research aimed to determine if microenvironmental metabolites are also altered in the leukemic BMME, and whether they contribute to an immunosuppressive microenvironment and cancer progression.

A hallmark of cancer is the “Warburg Effect”, the ongoing production of energy through aerobic glycolysis, even with fully functional mitochondrial oxidative phosphorylation (OXPHOS) (30). While AML subtypes, and even leukemic cells within an individual, are heterogeneous in their preferred metabolic route, many AML cells upregulate both glycolysis and OXPHOS, and leukemia cells are dependent on glycolysis for survival (31,32). In a final step of glycolysis, pyruvate is converted to lactate while the critical metabolic coenzyme NAD^+ is regenerated. The cell then exports lactate to the extracellular space. In noncancerous tissues, lactate is converted back to pyruvate by lactate dehydrogenase (LDH). However, the rate of lactate production by cancer cells exceeds this conversion by LDH, and lactate accumulates. Lactate concentrations have been reported to be elevated 5-30-fold in solid tumors and this correlates with poor prognosis (33,34). Recently, increased lactate in the BM during AML has been reported (35), though this is not yet well-documented. We hypothesized that metabolites including lactate accumulate in the AML BMME, driving immune suppression and leukemic progression.

Apart from a metabolic substrate, lactate itself acts as a signaling molecule through multiple routes. It is an extracellular ligand to the cell-surface “lactate sensor”, G-protein-coupled hydroxycarboxylic acid receptor 1 (GPR81/HCAR1) (36). GPR81 activation by lactate regulates cancer cell glycolysis, is crucial for cancer cell survival, and contributes to chemoresistance (37-39). Also, intracellular lactate levels are coordinated by import/export through monocarboxylate transporters (MCT)-1 and -4 (40,41). Inside the cell, lactate activates signaling pathways for stress and growth, such as transcription factor hypoxia-inducible factor-1 (HIF-1) and can be consumed as metabolic fuel via the TCA cycle (42). Targeting intracellular lactate by inhibiting MCT1/4 or LDH has been studied as a therapeutic approach for terminating AML cells, which may be more reliant on high rates of glycolysis than nonmalignant cell types in the BM (31,43). However, a drug targeting these key cellular proteins may have adverse effects on the nearby stressed hematopoietic system that also

relies on glycolysis and normal lactate transport for homeostasis. Therefore, a method to target lactate signaling in leukemia will be useful if it will spare the hematopoietic system.

GPR81 signaling has been linked to the pathophysiology of both cancer cells and the immune-suppressed tumor microenvironment. Downstream of GPR81 activation in cancer cells, pathways are upregulated for growth and survival, DNA repair proteins, chemoresistance via compound export (ex. ABCB1 transporter), and MCT1/4 expression (37-39). Increased GPR81-lactate signaling has dual immunoevasive effects, by upregulating PD-L1 on cancer cells, and dysregulating antigen-presenting cells in lung and breast cancers (44,45). It has also been reported that in leukocytes, such as macrophages, GPR81 inhibits NF-kB signaling and inflammasome activity (46). However, GPR81 signaling has not yet been studied in AML.

An immune-suppressed BM is well-known in AML, yet lactate has never been directly connected to this. Lactate signaling in tumors contributes to immunosuppressive tumor-associated macrophages (TAMs) that correlate with poor prognosis in multiple cancer types (33,47-52). Activation of macrophages to a classic/proinflammatory phenotype is marked by expression of inducible nitric oxide synthase (iNOS/Nos2), which mediates the cytotoxic production of NO to assist pathogen killing and phagocytosis, but suppressive macrophages are alternatively activated and instead express Arginase 1 (Arg1), the enzyme involved in depleting the substrate of iNOS, L-arginase (53,54). Alternative activation generally occurs during the resolution phase of an immune response such as wound healing, yet chronic immune signals in the cancer microenvironment cause macrophages to become polarized, rendering T cells less effective towards attack of cancer cells.

Recently, macrophages from AML BM have been found to be alternatively activated, have decreased phagocytosis, experimentally worsened leukemic transformation, and correlate with poor

prognosis (55,56). Repolarization of macrophages toward a more pro-inflammatory phenotype impacts disease state and survival time in murine models of AML (56,57). Still, little is known about the molecular mechanisms by which leukemia-associated macrophages (LAMs) are polarized to this phenotype and their specific functions. We hypothesized that elevated bone marrow lactate leads to polarization of LAMs to an immunosuppressive phenotype via GPR81. This research aimed to determine if, like solid tumors, lactate contributes to both a suppressive macrophage phenotype and direct support for AML cell growth and resistance pathways. Additionally, we investigated whether GPR81 signaling contributes to the pathologic loss of healthy blood cells observed in AML progression, and whether therapeutically targeting GPR81 would affect normal hematopoiesis.

Materials and Methods

Sampling of human bone marrow extracellular fluid

Deidentified bone marrow aspirates were collected from patients, and immediately centrifuged to remove cells. The supernatant was quickly taken to storage at -80°C until use. Patients were eligible if they were diagnosed *de novo* for AML, and other samples were taken from age- and sex-matched healthy controls.

Metabolomics by liquid chromatography coupled with mass spectrometry (LC/MS-MS)

See **Supplementary Methods**

Murine strains and AML model

All murine experiments were performed using male and female wild type C57BL/6J mice (RRID:IMSR_JAX:000664) or *Gpr81*$^{-/-}$ (GPR81KO) mice on the same background. Experiments

were performed using the following murine model of AML: A previously established model of blast crisis chronic myelogenous leukemia (bcCML) (23,58,59), an acutely progressing malignancy resulting in the accumulation of myeloid blasts in the BM. For more information on murine strains, ethics, and disease model generation, see **Supplementary Methods**.

Flow cytometry and fluorescence-activated cell sorting (FACS)

Bone marrow samples underwent red blood cell lysis prior to flow cytometric analyses (see **Supplementary Methods**)**.** All samples were resuspended in 1X phosphate-buffered saline (PBS) (Corning 21-040-CV) with added 2% heat-inactivated fetal bovine serum (htFBS) (Gibco 26140079, heat-treated at 56°C for 30 min). All antibodies for flow cytometry and cell sorting were obtained commercially. See **Supplementary Methods Table 1 (Table SM1)** for a list of flow cytometry antibodies and **Supplementary Methods Table 2 (Table SM2)** for markers and gating strategies used. Fluorescence minus one (FMO) prepared using cells, and positive controls prepared using UltraComp eBeads compensation beads (ThermoFisher Invitrogen 01-2222-42), were used in each experiment to ensure accurate staining and appropriate gating. Only the live, single cells were considered in analyses, where single cells were determined by side scatter and forward scatter, and live cells were distinguished by DAPI live/dead nuclear stain. Flow cytometric analyses were performed at the University of Rochester Wilmot Cancer Center on an LSRFortessa Cell Analyzer (BD Biosciences), and FACS was performed at the Flow Cytometry Core at the University of Rochester Medical Center on a FACSAria II system (BD Biosciences) with an 85-micron nozzle at 4°C, using FACSDiva software (BD Biosciences, RRID:SCR_001456), and then analyzed using FlowJo v10 software (BD Biosciences, RRID:SCR_008520).

Simplified Presentation of Incredibly Complex Evaluations (SPICE)

The SPICE analysis was performed using SPICE 6 software (RRID:SCR_016603) publicly available through the NIH NIAID site.

RNA sequencing (RNAseq)

RNA sequencing and analysis were performed by the University of Rochester Genomics Research Center. Demultiplexing, quality control, alignment, and analysis methods: Raw reads generated from the Illumina basecalls were demultiplexed using bcl2fastq version 2.19.1. Quality filtering and adapter removal are performed using FastP version 0.23.1 (RRID:SCR_016962) with the following parameters: "--length_required 35 --cut_front_window_size 1 --cut_front_mean_quality 13 --cut_front --cut_tail_window_size 1 --cut_tail_mean_quality 13 --cut_tail -y –r" (60). Processed/cleaned reads were then mapped to the GRCm39/gencode M31 reference using STAR_2.7.9a with the following parameters: "—twopass Mode Basic --runMode alignReads --outSAMtype BAM Unsorted – outSAMstrandField intronMotif --outFilterIntronMotifs RemoveNoncanonical –outReadsUnmapped Fastx" (61,62). Genelevel read quantification was derived using the subread-2.0.1 package (featureCounts, RRID:SCR_012919) with a GTF annotation file GRCm39/gencode M31, and the following parameters for stranded RNA libraries "-s 2 -t exon -g gene_name" (63). Differential expression analysis was performed using DESeq2-1.34.0 with a P-value threshold of 0.05 within R version 3.5.1 (https://www.R-project.org/) (64). A PCA plot was created within R using the pcaExplorer to measure sample expression variance (65). Heatmaps were generated using the pheatmap package (RRID:SCR_016418) using rLog transformed expression values (66). Gene ontology analyses were performed using the EnrichR package (RRID:SCR_001575) (67-69) Volcano plots and dot plots were created using ggplot2 (RRID:SCR_014601) (70).

Transcriptomic pathway analysis and GSEA

See **Supplementary Methods**

Macrophage cytokine profiling

To identify differential cytokines secreted by LAMs and normal macrophages: A stromal monolayer of murine whole bone marrow was grown in complete to confluency in “complete” (with 10% htFBS and 1x antibiotic-antimycotic (anti-anti) (Gibco 15240062)) Minimum Essential Medium α (MEM α) (with nucleosides and L-glutamine, without ascorbic acid, Gibco A10490-01). Macrophages were then sorted from nonleukemic mice or LAMs were sorted from bcCML mice via FACS. The macrophages were cocultured in the stromal monolayer dish for 4 days to establish a microenvironment, then the cell culture media was collected and stored immediately at -20C until use. The Proteome Profiler Mouse XL Cytokine Array (Bio-Techne (Minneapolis, MN, USA) R and D Systems ARY028) was used according to manufacturer protocol to perform an ELISA for a variety of cytokines. The blot was imaged using the ChemiDoc MP Imaging System (Bio-Rad (Hercules, CA, USA)) and Image Lab software (Bio-Rad) on the western blot high sensitivity setting for automatic exposure. Images were equally adjusted for background and the blot was qualitatively assessed for cytokine presence.

Bone marrow-derived macrophage (BMDM) production

Whole BM was plated in a vented tissue culture-treated 75cm^2 flask (NEST 708001) overnight in complete Dulbecco’s Modified Eagle Medium (DMEM) (Corning 10-013-CV). The next day, all non-adherent cells were transferred in the same culture media to be plated on 12-well cell culture dishes at 400,000 cells/well in 1 mL + recombinant murine macrophage colony-stimulating factor (M-CSF) (PeproTech 315-02), plus any treatment conditions. Media was changed on day 4 including stimuli/lactate, and differentiation to BMDMs was complete by day 7, where cells were either treated or grown/passaged up to P1.

Macrophage polarization experiments

Treatment groups were serum-starved for 6 hours before treatment (DMEM, anti-anti, and M-CSF without htFBS), and treatment conditions (100 ng/mL lipopolysaccharides (LPS) from E. coli O55:B5 (Sigma-Aldrich (St. Louis, MO, USA) L6529), or 5 ng/mL of recombinant murine interleukin (IL) -4 and -13 (IL-4, IL-13) (ILs) (ThermoFisher (Watham, MA, USA) PeproTech (Cranbury, NJ, USA) 214-14, 210-13), were added to the serum-free media for the time indicated. To remove cells for flow analysis, 0.25% trypsin-EDTA (ThermoFisher Gibco 25200056) was added for 5 min then cell scrapers were used. Additional syrosingopine (Sigma SML 1908, resuspended in DMSO) treatments were done at 5 µM. To determine if polarization is reversible, BMDMs were treated with polarization stimuli for 24 hours, then changed to fresh media and cultured for up to 48 hrs.

Quantitative real-time polymerase chain reaction (qRT-PCR)

Cells were grown to 70% confluency in corresponding media in tissue culture-treated 12-well plates. Media was changed to serum-free media for 12-24 hours before lactate treatment. Lactate was added to wells at 10 mmol/L and cells were cultured for the desired time. For BMDMs 5 ng/mL of IL4 and IL13 was also added to stimulate polarization. Wells were treated for 0, 1, 2, 4, 6, or 9 hours, and cells were then removed from the well by treatment with 0.25% trypsin-EDTA for three minutes then by the additional use of a cell-scraper for macrophage cultures. All cells were collected in an Eppendorf tube and centrifuged at 3000 x g for 3 minutes to pellet the cells. The supernatant was removed, and cells were resuspended in RLT lysis buffer (Qiagen), then stored at -20C until RNA extraction by RNeasy Plus Mini Kit (Qiagen 74134). The cDNA libraries were then prepared using the High-Capacity cDNA Reverse Transcription kit (Applied Biosystems, ThermoFisher 4368814). The TaqMan Gene Expression Master Mix (ThermoFisher 4369016) was used for qRT-PCR along with the following TaqMan Gene Expression Assays (FAM) (ThermoFisher 4331182): Gpr81/Hcar1

mouse (Mm00558586_s1), Mct1 mouse (Mm01306379_m1), Mct4 mouse (Mm01246825_m1), Arg1 mouse (Mm00475988_m1), iNOS mouse (Mm00440502_m1), and beta-actin mouse (Mm04394036_g1). The assay was run on the QuantStudio 12KFlex Real-Time PCR System at the UR Genomics Research Center. The relative quantification (RQ) of mRNA expression was calculated using the $2^{-(\Delta\Delta Ct)}$ method (Ct = cycle threshold).

Colony forming unit (CFU-C) assays

To plate cells for CFU-Cs, all cells were collected from the wells by collecting the media with non-adherent cells in a 15 mL conical tube, and then using 0.25% trypsin-EDTA on the adherent cells for five minutes then flushing the wells with fresh MEM α and adding it to the tube. Cells were pelleted by centrifugation for five minutes at 900 x g. Then, cells were resuspended in 0.5 mL of MEM α. From here, both 1:20 and 1:100 dilutions were made in 2.5 mL of media in separate Eppendorf tubes. Then, 0.2 mL of these dilutions were resuspended each in 2.5 mL aliquots of MethoCult (StemCell Technologies (Vancouver, CA) M3434) methylcellulose-containing media and immediately plated in duplicates of 1.2 mL into 35mm x 10mm sterile suspension culture dishes (Corning (Corning, NY, USA) 430588). These were placed inside a sterile 150 mm x 25 mm dish (NEST (Woodbridge, NJ, USA) 715001), with one open dish of sterile dH_20 in the center to retain humidity and prevent drying of the cultures. These were incubated for 10-14 days (5% CO_2; 37C), then colonies were counted using a microscope. For a description of experimental conditions see **Supplementary Methods**.

Additional Methods can be found in Supplementary Methods

Results

Extracellular metabolite levels are altered in bone marrow of AML patients, including elevated lactate

To profile the metabolite levels of the AML bone marrow microenvironment (BMME), we performed metabolomics on serum from bone marrow (BM) biopsies of AML patients at diagnosis, as well as healthy age- and sex-matched controls (**Fig. 1A**). The disease samples included different age, sex, and mutational subtypes (**Supplementary Table S1**). AML bone marrow displayed a general increase in extracellular metabolites (**Fig. 1B** and **1C**). Six metabolites were significantly altered during disease, listed in **Table 1,** and, of these, lactate was the most highly elevated. Lactate concentrations were measured to be approximately 2-5-fold higher in AML BM compared to controls (**Fig. 1D**). Collection of BM aspirate unavoidable dilutes the sample with peripheral blood, so actual lactate concentrations *in vivo* are likely greater than the reported concentrations.

Next, we aimed to identify a murine model to study lactate signaling in the leukemic BMME *in vivo*. We performed metabolomics on BM extracellular fluid from a murine model of blast-crisis chronic myelogenous leukemia (bcCML) (**Supplementary Fig. 1A**). BcCML cells contain translocation gene products BCR-ABL (Philadelphia chromosome) and NUP98-HOXA9 commonly found in myeloid leukemias and will engraft and then accumulate rapidly in the BM; this model of bcCML has been previously characterized and presents similarly to AML in humans (23,58,71-73). BcCML is especially useful in the study of the BMME because irradiation is not necessary to precondition the BM before transplantation of leukemic cells. Therefore, all changes observed in the microenvironment are without confounding effects of radiation. BcCML presented with elevated BM metabolites and lactate (**Supplementary Fig. 1B**). **Supplementary Table S2** lists the compounds with significantly altered levels. The lactate increase in the bcCML BM was relative to human AML BM (**Supplementary Fig. 1C** and **1D**), demonstrating that this model is well-suited to study elevated lactate in the AML BMME.

Leukemia-associated macrophages are alternatively activated to a CD206^{hi}, suppressive phenotype

We hypothesized that elevated lactate has a role in AML BM immune suppression through macrophage polarization, as it does in solid tumors. Using flow cytometry, we profiled the activation phenotype of leukemia-associated macrophages (LAMs) (Ly-6C^{-}, Ly-6G^{-}, CD45^{+}, F4/80^{+}) in the BM of bcCML mice, compared to nonleukemic (NL) controls (**Fig. 2B**). BcCML cells were distinguished from nonleukemic myeloid lineage cells by green fluorescent protein (GFP) co-expressed with the leukemic gene. Well-described macrophage activation markers were surveyed: classic/proinflammatory CD38 and major histocompatibility complex class II (MHCII) (74,75), and alternative/suppressive early growth response protein 2 (EGR2) and macrophage mannose receptor (MR/CD206) often found on tumor-associated macrophages (TAMs) (48,53,76-78). The software "Simplified Presentation of Incredibly Complex Evaluations" (SPICE 6.1) (NIH) was used to quantify the frequency of all combinations of macrophages based on the antibodies used. This unbiased approach identified a subset of LAMs increased in disease that overexpressed both CD206 and MHCII compared to NL macrophages (**Fig. 2B**), indicating a shift in macrophage subpopulations in the BM during leukemia. This subpopulation expressing both classic and alternative polarization markers reinforces the oversimplification of grouping macrophage activation states into M1/pro-and M2/anti-inflammatory based on markers (79), hence why we are not using the traditional M1-like and M2-like terminology herein.

Globally, there was an increase in the frequency of CD206^{hi} LAMs (**Fig. 2C**) and expression level of CD206 was increased on the CD206^{+} LAMs compared to NL macrophages (**Fig. 2D**), indicating a higher extent of polarization in LAMs compared to NL. The increase in CD206 was distinct to non-leukemia-derived (GFP^{-}) cells displaying the macrophage markers, and not from the myeloid

leukemia cells that display similar markers. CD206 was elevated throughout the disease course when >20% leukemia cells were present in the BM (**Supplementary Fig. 2A**). Despite the subset of LAMs identified by SPICE as increase in disease, the global frequency of macrophages positive for MHCII was lower in bcCML, and CD38 and EGR2 were unchanged (**Supplementary Fig. 2B-D**). The shift towards high CD206 and low MHCII on LAMs indicates an alternatively activated/suppressive phenotype. Interestingly, macrophages from leukemic spleen were less activated, supporting that the BM is the source of polarization stimuli (**Supplementary Fig. 2E-I**). An increase in CD206 was detectable on BM LAMs by an early stage of disease (7-10% leukemic cells in the BM) (**Supplementary Fig. 2J** and **2K**).

We further examined the functional phenotype of LAMs by transcriptional profiling. RNA sequencing (RNAseq) was performed on BM LAMs or NL controls. The LAM transcriptome was distinct from NL macrophages (**Fig. 2E** and **2F**). Top significantly downregulated Gene Ontology (GO) pathways identified by EnrichR analysis included neutrophil interactions and cell cycle control (**Supplementary Fig. 2L**). Top upregulated pathways were associated with regulation of immune and hematopoietic cells (**Supplementary Fig. 2M**). This supports an alternative function of LAMs, with a contribution to the immune-privileged and dysregulated hematopoietic BMME observed in AML. Proteome profiling detected several cytokines exclusively expressed by LAMs (**Fig. 2G** and **Table 2**). These cytokines have previously been implicated in solid tumors for an immunosuppressive microenvironment (CCL12, CCL6, PCSK9) (80,81), tumor cell proliferation and invasion (CXCL10) (82), immune cell chemotaxis (CCL12/MCP-5, CXCL10) (80,82), and tumor growth and metastasis (CXCL5/LIX, MMP3, proprotein convertase 9 (PCSK9)) (83-85).

To our knowledge, this is the first published transcriptomic dataset of murine TAMs from leukemic bone marrow. As such, we asked whether LAMs share transcriptional similarities/differences

with TAMs from other types of cancers. LAMs were compared and contrasted to murine F4/80$^+$ TAMs from solid tumors models of colorectal metastasis (CM) (86) and breast cancer (BC) (87) (accessed via the NIH National Center for Biotechnology Information (NCBI) Gene Expression Omnibus (GEO)). A pathway analysis identified common GO elements upregulated/downregulated in LAMs and TAMs compared to their internal controls (**Fig. 2H**). Common upregulated GO elements are listed in **Table 3**. Only two GO elements were common to LAMs and both types of TAMs. One was C-type lectin receptor (CLR) signaling, which functions in immunometabolism and macrophage polarization (88,89). CLRs recognize polysaccharides, namely from pathogens, and a notable CLR is the mannose receptor (MR) (90), also known as CD206, which we identified as elevated in LAMs. The other was nuclear casein kinase and cyclin-dependent kinase substrate 1 (NUCKS1), a nuclear DNA binding protein. NUCKS is a highly phosphorylated protein ubiquitously expressed in mice and humans, implicated in signal transduction related to the cell cycle and DNA damage response. NUCKS also regulates inflammation through NF-κβ mediated cytokine expression (91). Though NUCKS overexpression in various cancers has been reported (92,93), the role of NUCKS in macrophage polarization and function has not yet been studied.

LAMs shared an additional six common elements with TAMs from CM: tumor necrosis factor (TNF) and transforming growth factor β (TGF-β) signaling, two key pathways in immunomodulation generally related to T cells and the permissive cancer microenvironment (94-96); IRF8, involved in chronic inflammation, myeloid differentiation, and the activation of macrophages (97), and two parasite-response pathways. However, there were generally few common pathways between LAMs and TAMs. A greater number of downregulated elements were shared, the majority of which are related to the cell cycle (**Supplementary Table S3**), suggesting that augmented growth/replication occurs in cancer-associated macrophages from solid tumors and leukemic BM.

Then, to directly compare the LAM transcriptome to TAMs, gene set enrichment analyses (GSEA) were performed using “hallmark” gene sets from the Human Molecular Signatures Database (MSigDB), which are genes associated with well-defined biological states/pathways that have homology in mice and humans (**Fig. 2I**). **Table 4** lists the gene sets enriched in LAMs as compared to both CM and BC TAMs, these include cell growth and cell cycle control (MYC targets, E2F targets, DNA repair, G2M checkpoint, MTORC1 signaling, PI3K/AKT/mTOR pathway), cell metabolism (both OXPHOS and glycolysis, and fatty acid metabolism), allograft rejection, heme metabolism, and cell stress pathways (reactive oxygen species and unfolded protein response). Additionally, compared to CM TAMs, LAMs were enriched for the inflammatory signaling pathway IL2/STAT5 involved in the development of T_{Regs} and PD-L1 expression, recently reported in AML (35,98). LAMs were also enriched for the growth and cellular stress pathway PI3K/AKT/MTOR signaling (polarizes macrophages to an alternative phenotype (99)), protein secretion, the cell-cycle P53 pathway, and apoptosis (for a full list see **Supplementary Table S4**). Instead, gene sets enriched in both TAM types compared to LAMs included epithelial to mesenchymal transition and angiogenesis (**Fig. 2N**), which are functions more relevant to solid tumors. BC TAMs were also more enriched than LAMs for several inflammatory signaling pathways (see **Supplementary Table S5**). In all, LAMs are alternatively activated, yet they largely differ from TAMs and therefore should be separately investigated.

Lactate signaling through GPR81 contributes to the suppressive phenotype of leukemia-associated macrophages

Next, we addressed whether the increased BM lactate polarizes LAMs to the CD206^{hi}, suppressive phenotype. To isolate the effect of lactate, bone marrow-derived macrophages (BMDMs) were treated *in vitro* with physiologically relevant levels of lactate. To determine a physiologically relevant level we considered the following: BM extracellular lactate concentrations are likely higher *in vivo* than the measured mean concentration 4 mmol/L because AML patient BM biopsy samples are unavoidably

diluted by some peripheral blood upon collection. Also, we postulate that areas exist near AML cell-dense pockets that are higher in lactate concentration, as the BM is known to be spatially heterogeneous for concentrations of similar molecules, and pH (100). Therefore, 5-15 mmol/L of lactate was added for experiment treatments. As positive controls, we used lipopolysaccharide (LPS) as proinflammatory/ classic macrophage polarization stimuli, or interleukins (IL)-4 and -13 (IL-4, IL-13) as stimuli for alternative macrophage activation (101-104). IL-4/13 are well-described Type 2 helper T (Th2) cytokines produced in inflammatory responses such as tissue repair that persist during chronic type 2 inflammatory states, such as the AML BMME (105).

Polarization to CD206^{hi} BMDMs increased when lactate was combined with IL-4 and IL-13 (**Fig. 3A** and **3B**), compared to treatment with lactate or ILs alone. This indicated that lactate primes alternative macrophage polarization. Interestingly, the polarized state was nonpermanent, it reversed after the removal of stimuli for 48 hours (**Fig. 3C**). To assay for the functional phenotype of CD206^{hi} lactate-polarized BMDMs, we measured transcript levels of inducible nitric oxide synthase (*iNOS/Nos2*) which is expressed during a proinflammatory response, or Arginase 1 (*Arg1*) during a suppressive response. CD206^{hi} lactate-polarized BMDMs induced *Arg1* expression, and not *iNOS* (**Supplementary Fig. 3A** and **3B**). These findings support that CD206^{hi}macrophages in AML are suppressive and are sensitized to become alternatively activated by excess lactate.

To address which lactate signaling pathway results in alternative macrophage polarization *in vivo*, we considered available murine strains. Genetic knockout of MCT1 is embryonically lethal (106). While MCT4 knockout mice are viable (107), MCT1 would be present, and has a higher affinity for lactate (43). However, mice genetically lacking the lactate receptor GPR81 (*Gpr81*$^{-/-}$ or GPR81KO) grow to healthy adulthood, produce blood cells at a normal ratio, and have a similar weight and BM cellular density as wt mice (**Supplementary Fig. 3C-L**). Further, GPR81 has been implicated in the

suppressive cancer microenvironment in solid tumors (44,45). Therefore, we used GPR81KO mice to investigate the role of lactate-GPR81 signaling in LAM polarization *in vivo*. Wild type (wt) bcCML was initiated in GPR81KO mice, to eliminate GPR81 signaling from all non-leukemic BM cells (**Fig. 3D**). Elevated metabolites were also in the BM extracellular fluid from GPR81KO mice with bcCML (**Supplementary Fig. 3M**), supporting the use of this strain to study GPR81 signaling in the leukemic BMME.

We reinvestigated the polarization of LAMs in GPR81KO mice with bcCML. The increased frequency of macrophages in the BM observed in bcCML was partially reversed in GPR81KO mice (**Fig. 3E**). This suggests that GPR81 signaling regulates the growth/over proliferation of macrophages in disease. The LAMs in the GPR81KO BMME also expressed much lower CD206 levels, indicating that GPR81 promotes polarization of LAMs (**Fig. 3F** and **3G**). Further, the frequency of MHCII^{+} macrophages was higher (**Fig. 3H**), and the proinflammatory polarization marker CD38 was also increased in macrophages from GPR81KO mice (**Supplementary Fig. 3N**). GPR81KO mice displayed a similar leukemic burden in the BM as wild type by late-stage disease, however, there was a significant decrease in the peripheral blood and spleen (**Supplementary Fig. 3O-Q**), indicating a delay in disease course and/or a diminished peripheralization of leukemic blasts.

Assays for BMDM polarization *in vitro* confirmed the contribution of GPR81 signaling as a mechanism of LAM polarization. *Gpr81*$^{-/-}$ BMDMs did not upregulate CD206 as highly as wt BMDMs (**Fig. 3I** and **3J**). The range of *Arg1* expression also followed the trend of CD206 expression (**Supplementary Fig. 3R**). There was not a significant increase in the expression *Gpr81*, *Mct4, or iNOS,* though there was an increase in *Mct1* for only wt macrophages (**Supplementary Fig. 3S**). This suggests that GPR81 sensing of lactate induces upregulation of MCT1 for lactate import/export in macrophages. Other effects of GPR81 signaling are carried out by activation of the receptor and not

by changes in expression level of these related proteins. To assay for lactate import/export as an additional polarization mechanism, syrosingopine was used, a dual inhibitor of MCT1/4. A contribution of MCTs to polarization was observed (**Supplementary Fig. 3T-V**). Neither knockout of GPR81, inhibition of MCT1/4, nor combination of both completely blocked polarization, due to the strong stimulus with IL-4 and -13. Nevertheless, both intracellular and extracellular lactate signaling pathways contributed to macrophage polarization.

Lactate-GPR81 signaling drives leukemia cell growth and self-repopulation

We next investigated whether GPR81 signaling impacts myeloid leukemia cells, as it is known to be crucial for the survival of other types of cancer cells (38). *Gpr81*$^{-/-}$ bcCML cells were generated and then used to initiate disease either in wt mice or in GPR81KO mice (double-knockout (DKO)), where GPR81 signaling is not present on leukemic cells or in the BMME (**Fig. 4A**). Leukemic burden was largely reduced in the BM, peripheral blood, and spleen of by the time point of late-stage disease in GPR81KO DKO bcCML as compared to wt bcCML controls (**Fig. 4B-D**). There was a delayed rapid expansion of engrafted cells when GPR81KO bcCML cells were used (**Fig. 4E**), the leukemic burden was near zero at the time-point of early-stage disease when compared to wt bcCML cells (**Supplementary Fig. 4A-C**). The time to progression to >50% leukemic cells in the BM was significantly longer in GPR81 DKO compared to wt (**Fig. 4F**).

GPR81 is highly transcriptionally upregulated on some types of cancer cells, such as breast cancer (37). To assess the expression level of GPR81/*HCAR1* on human AML cells, analyses of publicly available RNA sequencing databases were performed. A dataset of BM from 707 AML patients, BeatAML 2.0 (accessed at vizome.org) (108), revealed that *HCAR1* is dysregulated in disease samples compared to healthy BM (**Supplementary Fig. 4D**). Further, 163 AML patient BM samples from The Cancer Genome Atlas (TCGA) Pan-Cancer Atlas database were analyzed

through cBioPortal for Cancer Genomics (accessed at cbioportal.org) (109). This dataset shows a rare subset of AML patient samples with “altered”/high GPR81/*HCAR1* mRNA expression greater than 2x, and these patients had a median survival time of 11 months less than those with “unaltered” *HCAR1* (5.03 vs 16.08 months) (**Supplementary Fig. 4E**). No gene mutations or structural variants of *HCAR1* were in AML subjects from TCGA datasets. This suggests that upregulation of GPR81 activity correlates with poor prognosis, though it is not largely overexpressed on AML cells.

As residual LSCs after chemotherapy are the primary reason for relapse in patients (25,26), we experimentally determined the impact of GPR81 signaling on LSC self-repopulation. When serial passaging in methylcellulose-containing media, *Gpr81*$^{-/-}$ bcCML cells produced fewer colonies on average at P0 and P1 and lost repopulating capacity by P2-P3, while wt bcCML cells continued to repopulate colonies to at least P7 (**Fig. 4G** and **4H**). Together, these data display the importance of GPR81 signaling to the rapid growth and self-repopulation of leukemia cells.

Elevated lactate is harmful to the hematopoietic bone marrow microenvironment

We considered that excess lactate in the BM may also be harmful to normal hematopoiesis. As we have previously reported, bcCML presented with an increase in the percentage of phenotypic hematopoietic stem and progenitor cells (HSPCs), also known as LSK cells, and multipotent progenitors (MPP): megakaryocyte-biased MPP2, myeloid-biased MPP3, and lymphoid-primed MPP4 (**Supplementary Fig. 5A-F,** see **Supplementary Methods Table SM2** for markers and gating strategies) (59). Also as previously reported, MSCs were expanded within the leukemic bone (23), a key stromal cell type for the maintenance of HSPCs; this was nonspecific to MSC subsets known to be important to HSC adhesion and self-renewal at the niche: PDGFRα/CD51 (PααV) or PDGFRα^{+}Sca-1^{+} (PαS) MSCs (**Supplementary Fig. 5G-I**) (110-112). Still, mature blood cell

populations are lost by late-stage bcCML (59), showing a dysfunction in progenitor cell maintenance and/or differentiation. Therefore, we investigated whether lactate impacts HSPCs and stromal cells.

To determine if lactate reduces the hematopoietic potential of HSPCs, colony-forming unit cell (CFU-C) assays (113,114) were performed. When treated with 10-15 mmol/L of lactate, HSPCs lost colony-forming potential after 72 hours (**Fig. 5A**). We asked if HSC-niche supportive stromal cells could increase the maintenance of HSPCs in the presence of lactate; CFU-C assays with lactate treatment were repeated on HSPCs cocultured with an adherent stromal monolayer (**Fig. 5B**). The stromal monolayer is grown from the adherent cells from whole BM and is composed of both a small percentage of MSCs (>1%, like the percentage seen in the bone *in vivo*) and macrophages (**Supplementary Fig. 5J** and **5K**). However, cocultures also showed reduced CFU-Cs (**Fig. 5C**), suggesting that stromal cells do not protect HSPCs from elevated lactate. Since we have previously reported that aged macrophages can alter the colony-forming potential of HSPCs (112), we tested the addition of LAMs to the cocultures compared to macrophages from NL mice rather than treatment by lactate (**Fig. 5D**). The HSPCs showed reduced CFU-Cs when cocultured with LAMs compared to healthy macrophages (**Fig. 5E**), suggesting that LAMs also provide altered hematopoietic maintenance signals compared to healthy BM macrophages.

We also asked whether lactate alters key stromal HSC niche cell types: MSCs and OBs. MSC cultures with lactate treatment produced fewer pre-OB colonies, and displayed reduced colony-forming ability to fibroblasts (CFU-F), a measure of MSC self-renewal potential (**Fig. 5F-H**). This is consistent with a loss of functional OBs and bone volume that we have previously reported as a pathophysiology of AML (23). These results highlight multiple damaging effects of elevated lactate on critical components of hematopoiesis in the BM.

Targeting GPR81 has modest protective effects on hematopoietic compartments

It will be important to determine whether targeting lactate in the BM via GPR81 will help or harm normal blood cell production and hematopoietic support. We posited that GPR81 may be largely dispensable to hematopoiesis, due to the fact that nonleukemic, adult *Gpr81*$^{-/-}$ mice have appropriate ratios of mature blood cells (**Supplementary Fig. 3C-H**). Next, we investigated whether hematopoietic populations are impacted by GPR81 signaling during pathologic conditions. The increased frequency of LSKs and short-term HSCs in bcCML was reversed when initiated in GPR81KO mice (**Fig. 6A-F**). Hematopoietic progenitor populations were otherwise unchanged. Frequencies of MSCs and OBs in bone were also unaffected (**Supplementary Fig. 6A-D**).

Additionally, we assayed whether GPR81 signaling is responsible for the reduction in colony-forming potential of HSPCs and MSCs by increased lactate. *Gpr81*$^{-/-}$ HSPCs showed a moderate reduction of CFU-C loss with or without a stromal monolayer compared to wild type (**Fig. 6G** and **6H**). However, lactate-treated *Gpr81*$^{-/-}$ MSCs still displayed a loss of pre-OBs and fibroblastic colonies (**Fig. 6I** and **6J**). Altogether, these data show that reducing GPR81 signaling has a positive impact on hematopoietic progenitors, without harmful effects to stromal support populations.

Discussion

Identifying novel therapeutic targets that consider the bone marrow microenvironment (BMME) as a whole is pertinent to improving AML treatment. Current chemotherapies commonly lead to relapse and are harsh on the noncancerous cells within the BM. Safe and effective immunotherapies for myeloid leukemias are still under development and pose the challenge of shared antigens with the myeloid immune cells. Herein, we report elevated levels of metabolites in the BMME during AML, defining excess lactate as a critical driver of AML-induced macrophage polarization and leukemia

progression. Using a bcCML model of AML and GPR81$^{-/-}$ mice, we identify GPR81 as a mechanism of leukemia-associated macrophage (LAM) polarization to a suppressive phenotype. Our results highlight the potential of GPR81 as a novel therapeutic target for both the leukemic suppression of the immune system and for AML cell self-repopulation. Additionally, knockout of GPR81 had mild preservative effects on the hematopoietic BMME during leukemia.

We conclude that GPR81 is a mechanism of polarization to CD206^{hi} LAMs during bcCML. CD206 is a known marker of suppressive TAMs in solid tumors associated with poor prognosis (48,76). Furthermore, CD206 has been recently suggested as a prognostic factor for AML (115) and is induced on monocytes cocultured with AML blasts (53). These findings, alongside our own, suggest that the polarization of LAMs is partly due to AML-cell secretion of lactate and that LAMs are the source of the CD206 linked to poor prognosis. Overall, LAMs also had lower MHCII expression, which is important for antigen presentation. However, SPICE analysis (NIH) identified an increased subpopulation in disease where both CD206 and MHCII were co-expressed. Future research should determine if there are specific functions of these subpopulations (CD206^{hi}/MHCII^{lo} vs. CD206^{+}/MHCII^{+}). Cytokines that LAMs secreted that healthy nonleukemic bone marrow macrophages did not were associated with immunosuppression, lymphocyte trafficking, and cancer growth and metastasis. This offers future opportunities to confirm the role of each of these cytokines in the BMME during AML. As the polarized state was reversible, there is potential for therapeutic repolarization of LAMs to increase the efficacy of chemotherapies or other immunotherapies, such as CAR-T cell therapy.

Others have reported a role of the intracellular signaling cascades of GPR81 in anti-inflammatory-like macrophage polarization (47). One way by which GPR81 signals is by reducing cyclic AMP (cAMP)/cAMP-dependent protein kinase A (PKA), leading to decreased activation of

cAMP-response element binding (CREB) transcription factor (116). CREB is ubiquitously expressed and responsively induces genes associated with cell proliferation, differentiation, survival, and macrophage polarization to an M2-like/alternative phenotype (117,118). The mechanism of polarization can be confirmed by determining whether the same signaling pathways downstream of GPR81 are responsible for LAM phenotypes.

Comparative transcriptomic analysis found few shared common elements between LAMs and TAMs, highlighting LAMs as a unique type of cancer-associated macrophage. Upregulation of CLR signaling (such as CD206) was displayed by all. Shared downregulated elements related to cell cycle control may explain an increased frequency of macrophages in the leukemic bone marrow (**Fig. 3E**). LAMs were enriched for cell metabolism, cell stress pathways, and immune regulation compared to TAMs. Shifts in metabolism can influence phenotypes that are energy-sensitive, for example, the activation phenotype of macrophages. Generally, proinflammatory and phagocytic macrophages have higher energy demands and shift to glycolysis upon activation, while alternative/suppressive and non-activated macrophages preferentially use OXPHOS (119). LAMs were enriched for both glycolysis and OXPHOS compared to other types of TAMs, yet still display an alternative phenotype.

A recent study by Weinhäuser et al. performed single-cell RNA sequencing on human AML-associated macrophages (AAMs), and reported heterogeneity, alternative polarization, and overexpression of CD206, similar to our findings on LAMs (55). The human alternatively polarized macrophages correlated with poor prognosis in a cohort of MDS patients and influenced engraftment of patient-derived xerographs. Also, our GSEA analysis reflected the altered transcriptional program in these AAMs, with upregulated mitochondrial function including fatty acid oxidation, and NAD+ generation, which is associated with converting pyruvate to lactate. This suggests that the upregulation of glycolysis by macrophages may be an additional source of excess lactate in the BM

during AML. The similarity of our LAM findings to these human AAMs highlights the translatability of our model and findings to human AML. However, while data from Weinhäuser et al. suggested that the alternative functionality of AAMs that were not derived from the leukemic clone is in part due to the acquisition of AML-like mutations, our research demonstrates that the polarization phenotype of non-leukemia-derived macrophages can also occur solely due to alterations to the microenvironment.

Our unbiased metabolomics screening identified lactate as the most elevated extracellular metabolite in the BMME during AML, which has been identified as having the strongest prognostic risk value of metabolites detected in the serum from cytogenetically normal AML patients (120). The second most altered metabolite was citrulline, which was depleted. This may be a result of the citrulline-arginine cycle during prolonged production of nitric oxide (NO) by proinflammatory macrophages (121). Of the additional four significantly increased metabolites that we identified, serine has been previously connected to AML cell survival (122), while dihydroxyacetone phosphate (DHAP), ribose-P, and ornithine are intermediates in metabolic reactions and can be further studied for their influence on AML progression. To note, an amino acid-enriched BMME was observed during bcCML, and amino acids are critical for cancer cells to thrive (27,123); the reason or source of the extra amino acids is yet to be determined.

Our research also supports the further study of T cell suppression in AML, induced through secretion of cytokines from LAMs and directly by lactate. Interestingly, regulatory T cells (T_{Regs}), which are inhibitory to T cells, are more resistant to lactate-mediated inhibition than other T cell types (124), and are increased in AML patients (125). Furthermore, alternatively activated macrophages induce chemotaxis/differentiation of T_{Regs} which further the pro-tumor microenvironment (81,126,127). At the hematopoietic niche, T_{regs} provide an immune-suppressed niche where LSCs may escape immune attack (128). Lactate can directly affect interactions between cancer cells and T cells, leading to CD8+

T cell exhaustion, suppression of MHCII^{hi} immune cells and tumor-infiltrating T-cells, and expression of PD-L1 on tumor cells (45,129). The impact of lactate and GPR81 signaling on T cell subsets in the BM has not yet been studied.

Relapse following chemotherapy is currently one of the greatest hurdles in treating AML. GPR81 reduced the repopulation capacity of leukemia cells and extended survival time in our model. The signaling pathways downstream of GPR81 are numerous, and multiple pathways have been investigated in cancer cell metabolism, DNA repair, and chemoresistance (37-39). Defining the signaling pathways downstream of GPR81 in AML and other hematopoietic malignancies is promising for identifying additional mechanisms to target LSCs in the BM.

Alterations to the BMME and the loss of normal hematopoiesis lead to fatal complications of the disease. Unfortunately, most current treatment options for AML exacerbate this. Therefore, novel therapeutic targets for AML must also be investigated for effects on the hematopoietic BMME. The experimental knockout of GPR81 described herein exhibited a protective effect of inhibiting GPR81 signaling in the leukemic BM, on the inappropriate expansion of HSPC populations that may lead to their exhaustion. However, this data shows that GPR81 is not the only signaling mechanism by which lactate harms HSPCs and stromal support.

Limitations of this study include the use of an acute murine myeloid leukemia model in which the disease state progresses extremely rapidly, and therefore, may miss some long-term harm to the BM caused by chronically elevated lactate. Also, repolarization of LAMs did not cause a detectable change in the leukemic burden in the BM during this acute model but was detectable in the spleen and peripheral blood. This is interesting because macrophage depletion has been found to promote mobilization of HSCs (16). Further research is needed to determine if the excess of macrophages in

the BM promotes retention of HSCs/LSCs at the niche. If so, does this increase the escape of chemotherapeutic treatment? Other limitations include the lack of a specific inhibitor to GPR81 to replicate assays on human macrophages or human AML cell models. Future research may leverage siRNA or CRISPR-Cas9 systems to knock out GPR81 in human cells. This study supports the development of a specific GPR81 antagonist, both for research and translational use as a therapeutic.

In conclusion, this research suggests that targeting GPR81 signaling in the BMME during AML may be a selective and well-tolerated therapeutic option to prevent LSC repopulation and rescue microenvironmental dysfunction. GPR81 has the unique potential of dual targeting to immune and cancer cells. Additionally, as lactate production is a hallmark of cancer, findings on the mechanisms of lactate signaling to immune and hematopoietic cells within the BMME are potentially applicable to multiple malignancies with BM involvement, including additional types of leukemia as well as bone metastases of solid tumors.

Acknowledgments:

Financial support for this project came from the Wilmot Cancer Institute Research Development Funding Program Pilot Award to Dr. Frisch and Dr. Munger, an American Cancer Society Grant RSG-22-165-01-MM to Dr. Frisch, and from a National Research Service Award (NRSA) Institutional Research Training Grant (T32) 5T32AR076950-03 from the National Institutes of Health (NIH) to Dr. Soto through the Rochester Musculoskeletal (ROCMSK) Training Program at the University of Rochester Center for Musculoskeletal Research (CMSR).

We would like to acknowledge: Dr. Vadivel Ganapathy, Ph.D. at Texas Tech University for kindly gifting the *Gpr81*$^{-/-}$ mice, the Genomics Research Center at the University of Rochester Medical Center for RNA sequencing and analysis, the flow cytometry core for FACS, and Dr. Helene

McMurray, Ph.D. at the University of Rochester School of Medicine and Dentistry for insight on accessing and analyzing publicly available data from cancer patient databases.

Data Availability Statement: The metabolomic datasets generated and analyzed during the study, and any other raw data, are available from the corresponding author upon request. The transcriptomic datasets will be made publicly available on GEO upon publication.

References:

1. Ferrara F, Schiffer CA. Acute myeloid leukaemia in adults. The Lancet **2013**;381(9865):484-95 doi https://doi.org/10.1016/S0140-6736(12)61727-9.
2. Döhner H, Weisdorf DJ, Bloomfield CD. Acute Myeloid Leukemia. New England Journal of Medicine **2015**;373(12):1136-52 doi 10.1056/NEJMra1406184.
3. Chang H-Y, Rodriguez V, Narboni G, Bodey GP, Luna MA, Freireich EJ. CAUSES OF DEATH IN ADULTS WITH ACUTE LEUKEMIA. Medicine **1976**;55(3).
4. Miraki-Moud F, Anjos-Afonso F, Hodby KA, Griessinger E, Rosignoli G, Lillington D*, et al.* Acute myeloid leukemia does not deplete normal hematopoietic stem cells but induces cytopenias by impeding their differentiation. Proceedings of the National Academy of Sciences of the United States of America **2013**;110(33):13576-81 doi 10.1073/pnas.1301891110.
5. Crossnohere NL, Richardson DR, Reinhart C, O'Donoghue B, Love SM, Smith BD*, et al.* Side effects from acute myeloid leukemia treatment: results from a national survey. Current Medical Research and Opinion **2019**;35(11):1965-70 doi 10.1080/03007995.2019.1631149.
6. Thol F, Ganser A. Treatment of Relapsed Acute Myeloid Leukemia. Current Treatment Options in Oncology **2020**;21(8):66 doi 10.1007/s11864-020-00765-5.
7. Yi M, Li A, Zhou L, Chu Q, Song Y, Wu K. The global burden and attributable risk factor analysis of acute myeloid leukemia in 195 countries and territories from 1990 to 2017: estimates based on the global burden of disease study 2017. Journal of Hematology & Oncology **2020**;13(1):72 doi 10.1186/s13045-020-00908-z.

8. Isidori A, Cerchione C, Daver N, DiNardo C, Garcia-Manero G, Konopleva M*, et al.* Immunotherapy in Acute Myeloid Leukemia: Where We Stand. Frontiers in Oncology **2021**;11 doi 10.3389/fonc.2021.656218.

9. Greenbaum A, Hsu Y-MS, Day RB, Schuettpelz LG, Christopher MJ, Borgerding JN*, et al.* CXCL12 in early mesenchymal progenitors is required for haematopoietic stem-cell maintenance. Nature **2013**;495(7440):227-30 doi 10.1038/nature11926.

10. Méndez-Ferrer S, Michurina TV, Ferraro F, Mazloom AR, MacArthur BD, Lira SA*, et al.* Mesenchymal and haematopoietic stem cells form a unique bone marrow niche. Nature **2010**;466(7308):829-34 doi 10.1038/nature09262.

11. Calvi LM, Adams GB, Weibrecht KW, Weber JM, Olson DP, Knight MC*, et al.* Osteoblastic cells regulate the haematopoietic stem cell niche. Nature **2003**;425(6960):841-6 doi 10.1038/nature02040.

12. Zhu J, Garrett R, Jung Y, Zhang Y, Kim N, Wang J*, et al.* Osteoblasts support B-lymphocyte commitment and differentiation from hematopoietic stem cells. Blood **2007**;109(9):3706-12 doi 10.1182/blood-2006-08-041384.

13. Kunisaki Y, Bruns I, Scheiermann C, Ahmed J, Pinho S, Zhang D*, et al.* Arteriolar niches maintain haematopoietic stem cell quiescence. Nature **2013**;502(7473):637-43 doi 10.1038/nature12612.

14. Acar M, Kocherlakota KS, Murphy MM, Peyer JG, Oguro H, Inra CN*, et al.* Deep imaging of bone marrow shows non-dividing stem cells are mainly perisinusoidal. Nature **2015**;526(7571):126-30 doi 10.1038/nature15250.

15. Fang S, Chen S, Nurmi H, Leppänen V-M, Jeltsch M, Scadden D*, et al.* VEGF-C protects the integrity of the bone marrow perivascular niche in mice. Blood **2020**;136(16):1871-83 doi 10.1182/blood.2020005699.

16. Chow A, Lucas D, Hidalgo A, Méndez-Ferrer S, Hashimoto D, Scheiermann C*, et al.* Bone marrow CD169+ macrophages promote the retention of hematopoietic stem and progenitor cells in the mesenchymal stem cell niche. Journal of Experimental Medicine **2011**;208(2):261-71 doi 10.1084/jem.20101688.

17. Staversky RJ, Byun DK, Georger MA, Zaffuto BJ, Goodman A, Becker MW*, et al.* The Chemokine CCL3 Regulates Myeloid Differentiation and Hematopoietic Stem Cell Numbers. Sci Rep **2018**;8(1):14691 doi 10.1038/s41598-018-32978-y.

18. Sitnicka E, Lin N, Priestley G, Fox N, Broudy V, Wolf N, *et al.* The effect of thrombopoietin on the proliferation and differentiation of murine hematopoietic stem cells. Blood **1996**;87(12):4998-5005 doi 10.1182/blood.V87.12.4998.bloodjournal87124998.

19. Arai F, Hirao A, Ohmura M, Sato H, Matsuoka S, Takubo K, *et al.* Tie2/angiopoietin-1 signaling regulates hematopoietic stem cell quiescence in the bone marrow niche. Cell **2004**;118(2):149-61 doi 10.1016/j.cell.2004.07.004.

20. Goncalves KA, Silberstein L, Li S, Severe N, Hu MG, Yang H, *et al.* Angiogenin Promotes Hematopoietic Regeneration by Dichotomously Regulating Quiescence of Stem and Progenitor Cells. Cell **2016**;166(4):894-906 doi 10.1016/j.cell.2016.06.042.

21. Winkler IG, Barbier V, Nowlan B, Jacobsen RN, Forristal CE, Patton JT, *et al.* Vascular niche E-selectin regulates hematopoietic stem cell dormancy, self renewal and chemoresistance. Nat Med **2012**;18(11):1651-7 doi 10.1038/nm.2969.

22. Kode A, Manavalan JS, Mosialou I, Bhagat G, Rathinam CV, Luo N, *et al.* Leukaemogenesis induced by an activating β-catenin mutation in osteoblasts. Nature **2014**;506(7487):240-4 doi 10.1038/nature12883.

23. Frisch BJ, Ashton JM, Xing L, Becker MW, Jordan CT, Calvi LM. Functional inhibition of osteoblastic cells in an in vivo mouse model of myeloid leukemia. Blood **2012**;119(2):540-50 doi 10.1182/blood-2011-04-348151.

24. Soto CA, Lo Celso C, Purton LE, Frisch BJ. From the niche to malignant hematopoiesis and back: reciprocal interactions between leukemia and the bone marrow microenvironment. JBMR Plus **2021**;5(10):e10516 doi https://doi.org/10.1002/jbm4.10516.

25. Ishikawa F, Yoshida S, Saito Y, Hijikata A, Kitamura H, Tanaka S, *et al.* Chemotherapy-resistant human AML stem cells home to and engraft within the bone-marrow endosteal region. Nature Biotechnology **2007**;25(11):1315-21 doi 10.1038/nbt1350.

26. Lapidot T, Sirard C, Vormoor J, Murdoch B, Hoang T, Caceres-Cortes J, *et al.* A cell initiating human acute myeloid leukaemia after transplantation into SCID mice. Nature **1994**;367(6464):645-8 doi 10.1038/367645a0.

27. Bader JE, Voss K, Rathmell JC. Targeting Metabolism to Improve the Tumor Microenvironment for Cancer Immunotherapy. Molecular Cell **2020**;78(6):1019-33 doi https://doi.org/10.1016/j.molcel.2020.05.034.

28. Bejarano L, Jordão MJC, Joyce JA. Therapeutic Targeting of the Tumor Microenvironment. Cancer Discov **2021**;11(4):933-59 doi 10.1158/2159-8290.Cd-20-1808.

29. Elia I, Haigis MC. Metabolites and the tumour microenvironment: from cellular mechanisms to systemic metabolism. Nature Metabolism **2021**;3(1):21-32 doi 10.1038/s42255-020-00317-z.
30. Warburg O. On the origin of cancer cells. Science **1956**;123(3191):309-14 doi 10.1126/science.123.3191.309.
31. Wang Y-H, Israelsen William J, Lee D, Yu Vionnie WC, Jeanson Nathaniel T, Clish Clary B*, et al.* Cell-State-Specific Metabolic Dependency in Hematopoiesis and Leukemogenesis. Cell **2014**;158(6):1309-23 doi https://doi.org/10.1016/j.cell.2014.07.048.
32. Erdem A, Marin S, Pereira-Martins DA, Cortés R, Cunningham A, Pruis MG*, et al.* The Glycolytic Gatekeeper PDK1 defines different metabolic states between genetically distinct subtypes of human acute myeloid leukemia. Nat Commun **2022**;13(1):1105 doi 10.1038/s41467-022-28737-3.
33. de la Cruz-López KG, Castro-Muñoz LJ, Reyes-Hernández DO, García-Carrancá A, Manzo-Merino J. Lactate in the Regulation of Tumor Microenvironment and Therapeutic Approaches. Frontiers in oncology **2019**;9:1143- doi 10.3389/fonc.2019.01143.
34. Walenta S, Wetterling M, Lehrke M, Schwickert G, Sundfør K, Rofstad EK*, et al.* High lactate levels predict likelihood of metastases, tumor recurrence, and restricted patient survival in human cervical cancers. Cancer Res **2000**;60(4):916-21.
35. Huang Z-W, Zhang X-N, Zhang L, Liu L-L, Zhang J-W, Sun Y-X*, et al.* STAT5 promotes PD-L1 expression by facilitating histone lactylation to drive immunosuppression in acute myeloid leukemia. Signal Transduction and Targeted Therapy **2023**;8(1):391 doi 10.1038/s41392-023-01605-2.
36. Lee DK, Nguyen T, Lynch KR, Cheng R, Vanti WB, Arkhitko O*, et al.* Discovery and mapping of ten novel G protein-coupled receptor genes. Gene **2001**;275(1):83-91 doi https://doi.org/10.1016/S0378-1119(01)00651-5.
37. Ishihara S, Hata K, Hirose K, Okui T, Toyosawa S, Uzawa N*, et al.* The lactate sensor GPR81 regulates glycolysis and tumor growth of breast cancer. Scientific Reports **2022**;12(1):6261 doi 10.1038/s41598-022-10143-w.
38. Roland CL, Arumugam T, Deng D, Liu SH, Philip B, Gomez S*, et al.* Cell surface lactate receptor GPR81 is crucial for cancer cell survival. Cancer Res **2014**;74(18):5301-10 doi 10.1158/0008-5472.Can-14-0319.
39. Wagner W, Kania KD, Blauz A, Ciszewski WM. The lactate receptor (HCAR1/GPR81) contributes to doxorubicin chemoresistance via abcb1 transporter up-regulation in human cervical cancer hela cells. Journal of Physiology and Pharmacology **2017**;68(4):555-64.

40. Ritzhaupt A, Wood IS, Ellis A, Hosie KB, Shirazi-Beechey SP. Identification and characterization of a monocarboxylate transporter (MCT1) in pig and human colon: its potential to transport l-lactate as well as butyrate. The Journal of Physiology **1998**;513(3):719-32 doi https://doi.org/10.1111/j.1469-7793.1998.719ba.x.

41. Dimmer K-S, Friedrich B, Lang F, Deitmer JW, Broer S. The low-affinity monocarboxylate transporter MCT4 is adapted to the export of lactate in highly glycolytic cells. Biochemical Journal **2000**;350(1):219-27 doi 10.1042/bj3500219.

42. Li X, Yang Y, Zhang B, Lin X, Fu X, An Y*, et al.* Lactate metabolism in human health and disease. Signal Transduction and Targeted Therapy **2022**;7(1):305 doi 10.1038/s41392-022-01151-3.

43. Benjamin D, Robay D, Hindupur SK, Pohlmann J, Colombi M, El-Shemerly MY*, et al.* Dual Inhibition of the Lactate Transporters MCT1 and MCT4 Is Synthetic Lethal with Metformin due to NAD+ Depletion in Cancer Cells. Cell Rep **2018**;25(11):3047-58.e4 doi 10.1016/j.celrep.2018.11.043.

44. Feng J, Yang H, Zhang Y, Wei H, Zhu Z, Zhu B*, et al.* Tumor cell-derived lactate induces TAZ-dependent upregulation of PD-L1 through GPR81 in human lung cancer cells. Oncogene **2017**;36(42):5829-39 doi 10.1038/onc.2017.188.

45. Brown TP, Bhattacharjee P, Ramachandran S, Sivaprakasam S, Ristic B, Sikder MOF*, et al.* The lactate receptor GPR81 promotes breast cancer growth via a paracrine mechanism involving antigen-presenting cells in the tumor microenvironment. Oncogene **2020**;39(16):3292-304 doi 10.1038/s41388-020-1216-5.

46. Hoque R, Farooq A, Ghani A, Gorelick F, Mehal WZ. Lactate Reduces Liver and Pancreatic Injury in Toll-Like Receptor– and Inflammasome-Mediated Inflammation via GPR81-Mediated Suppression of Innate Immunity. Gastroenterology **2014**;146(7):1763-74 doi https://doi.org/10.1053/j.gastro.2014.03.014.

47. Zhou H-c, Yan X-y, Yu W-w, Liang X-q, Du X-y, Liu Z-c*, et al.* Lactic acid in macrophage polarization: The significant role in inflammation and cancer. International Reviews of Immunology **2022**;41(1):4-18 doi 10.1080/08830185.2021.1955876.

48. Jaynes JM, Sable R, Ronzetti M, Bautista W, Knotts Z, Abisoye-Ogunniyan A*, et al.* Mannose receptor (CD206) activation in tumor-associated macrophages enhances adaptive and innate antitumor immune responses. Science Translational Medicine **2020**;12(530):eaax6337 doi 10.1126/scitranslmed.aax6337.

49. Gordon S, Martinez FO. Alternative Activation of Macrophages: Mechanism and Functions. Immunity **2010**;32(5):593-604 doi https://doi.org/10.1016/j.immuni.2010.05.007.

50. Colegio OR, Chu N-Q, Szabo AL, Chu T, Rhebergen AM, Jairam V*, et al.* Functional polarization of tumour-associated macrophages by tumour-derived lactic acid. Nature **2014**;513(7519):559-63 doi 10.1038/nature13490.

51. Zhang Q, He Y, Luo N, Patel SJ, Han Y, Gao R*, et al.* Landscape and Dynamics of Single Immune Cells in Hepatocellular Carcinoma. Cell **2019**;179(4):829-45.e20 doi https://doi.org/10.1016/j.cell.2019.10.003.

52. Su X, Xu Y, Fox GC, Xiang J, Kwakwa KA, Davis JL*, et al.* Breast cancer-derived GM-CSF regulates arginase 1 in myeloid cells to promote an immunosuppressive microenvironment. J Clin Invest **2021**;131(20) doi 10.1172/jci145296.

53. Mussai F, De Santo C, Abu-Dayyeh I, Booth S, Quek L, McEwen-Smith RM*, et al.* Acute myeloid leukemia creates an arginase-dependent immunosuppressive microenvironment. Blood **2013**;122(5):749-58 doi 10.1182/blood-2013-01-480129.

54. Bailey JD, Diotallevi M, Nicol T, McNeill E, Shaw A, Chuaiphichai S*, et al.* Nitric Oxide Modulates Metabolic Remodeling in Inflammatory Macrophages through TCA Cycle Regulation and Itaconate Accumulation. Cell Reports **2019**;28(1):218-30.e7 doi https://doi.org/10.1016/j.celrep.2019.06.018.

55. Weinhäuser I, Pereira-Martins DA, Almeida LY, Hilberink JR, Silveira DRA, Quek L*, et al.* M2 macrophages drive leukemic transformation by imposing resistance to phagocytosis and improving mitochondrial metabolism. Science Advances **2023**;9(15):eadf8522 doi doi:10.1126/sciadv.adf8522.

56. Yang X, Feng W, Wang R, Yang F, Wang L, Chen S*, et al.* Repolarizing heterogeneous leukemia-associated macrophages with more M1 characteristics eliminates their pro-leukemic effects. Oncoimmunology **2018**;7(4):e1412910 doi 10.1080/2162402x.2017.1412910.

57. Al-Matary YS, Botezatu L, Opalka B, Hönes JM, Lams RF, Thivakaran A*, et al.* Acute myeloid leukemia cells polarize macrophages towards a leukemia supporting state in a Growth factor independence 1 dependent manner. Haematologica **2016**;101(10):1216-27 doi 10.3324/haematol.2016.143180.

58. Neering SJ, Bushnell T, Sozer S, Ashton J, Rossi RM, Wang P-Y*, et al.* Leukemia stem cells in a genetically defined murine model of blast-crisis CML. Blood **2007**;110(7):2578-85 doi 10.1182/blood-2007-02-073031.

59. Ackun-Farmmer MA, Soto CA, Lesch ML, Byun D, Yang L, Calvi LM*, et al.* Reduction of leukemic burden via bone-targeted nanoparticle delivery of an inhibitor of C-chemokine (C-C motif) ligand 3 (CCL3) signaling. Faseb j **2021**;35(4):e21402 doi 10.1096/fj.202000938RR.
60. Chen S, Zhou Y, Chen Y, Gu J. fastp: an ultra-fast all-in-one FASTQ preprocessor. Bioinformatics **2018**;34(17):i884-i90 doi 10.1093/bioinformatics/bty560.
61. Frankish A, Diekhans M, Jungreis I, Lagarde J, Loveland Jane E, Mudge JM*, et al.* GENCODE 2021. Nucleic Acids Research **2020**;49(D1):D916-D23 doi 10.1093/nar/gkaa1087.
62. Dobin A, Davis CA, Schlesinger F, Drenkow J, Zaleski C, Jha S*, et al.* STAR: ultrafast universal RNA-seq aligner. Bioinformatics **2012**;29(1):15-21 doi 10.1093/bioinformatics/bts635.
63. Liao Y, Smyth GK, Shi W. The R package Rsubread is easier, faster, cheaper and better for alignment and quantification of RNA sequencing reads. Nucleic Acids Research **2019**;47(8):e47-e doi 10.1093/nar/gkz114.
64. Love MI, Huber W, Anders S. Moderated estimation of fold change and dispersion for RNA-seq data with DESeq2. Genome Biology **2014**;15(12):550 doi 10.1186/s13059-014-0550-8.
65. Marini F, Binder H. pcaExplorer: an R/Bioconductor package for interacting with RNA-seq principal components. BMC Bioinformatics **2019**;20(1):331 doi 10.1186/s12859-019-2879-1.
66. Kolde R. Package ‘pheatmap’. Version 1.0.12.
67. Chen EY, Tan CM, Kou Y, Duan Q, Wang Z, Meirelles GV*, et al.* Enrichr: interactive and collaborative HTML5 gene list enrichment analysis tool. BMC Bioinformatics **2013**;14(1):128 doi 10.1186/1471-2105-14-128.
68. Kuleshov MV, Jones MR, Rouillard AD, Fernandez NF, Duan Q, Wang Z*, et al.* Enrichr: a comprehensive gene set enrichment analysis web server 2016 update. Nucleic Acids Research **2016**;44(W1):W90-W7 doi 10.1093/nar/gkw377.
69. Xie Z, Bailey A, Kuleshov MV, Clarke DJB, Evangelista JE, Jenkins SL*, et al.* Gene Set Knowledge Discovery with Enrichr. Current Protocols **2021**;1(3):e90 doi https://doi.org/10.1002/cpz1.90.
70. Wickham H. ggplot2: Elegant Graphics for Data Analysis. Springer-Verlag New York; 2016.
71. Yamamoto K, Nakamura Y, Nakamura Y, Saito K, Furusawa S. Expression of the NUP98/HOXA9 fusion transcript in the blast crisis of Philadelphia chromosome-positive chronic myelogenous leukaemia with t(7;11)(p15;p15). British Journal of Haematology **2000**;109(2):423-6 doi 10.1046/j.1365-2141.2000.02003.x.

72. Kroon E, Thorsteinsdottir U, Mayotte N, Nakamura T, Sauvageau G. NUP98-HOXA9 expression in hemopoietic stem cells induces chronic and acute myeloid leukemias in mice. Embo j **2001**;20(3):350-61 doi 10.1093/emboj/20.3.350.
73. Ren R. Mechanisms of BCR–ABL in the pathogenesis of chronic myelogenous leukaemia. Nature Reviews Cancer **2005**;5(3):172-83 doi 10.1038/nrc1567.
74. Li W, Li Y, Jin X, Liao Q, Chen Z, Peng H*, et al.* CD38: A Significant Regulator of Macrophage Function. Front Oncol **2022**;12:775649 doi 10.3389/fonc.2022.775649.
75. Chávez-Galán L, Olleros ML, Vesin D, Garcia I. Much More than M1 and M2 Macrophages, There are also CD169+ and TCR+ Macrophages. Frontiers in Immunology **2015**;6 doi 10.3389/fimmu.2015.00263.
76. Heng Y, Zhu X, Lin H, jingyu M, Ding X, Tao L*, et al.* CD206+ tumor-associated macrophages interact with CD4+ tumor-infiltrating lymphocytes and predict adverse patient outcome in human laryngeal squamous cell carcinoma. Journal of Translational Medicine **2023**;21(1):167 doi 10.1186/s12967-023-03910-4.
77. Modak M, Mattes A-K, Reiss D, Skronska-Wasek W, Langlois R, Sabarth N*, et al.* CD206+ tumor-associated macrophages cross-present tumor antigen and drive antitumor immunity. JCI Insight **2022**;7(11) doi 10.1172/jci.insight.155022.
78. Veremeyko T, Yung AWY, Anthony DC, Strekalova T, Ponomarev ED. Early Growth Response Gene-2 Is Essential for M1 and M2 Macrophage Activation and Plasticity by Modulation of the Transcription Factor CEBPβ. Frontiers in Immunology **2018**;9 doi 10.3389/fimmu.2018.02515.
79. Pan Y, Yu Y, Wang X, Zhang T. Tumor-Associated Macrophages in Tumor Immunity. Frontiers in Immunology **2020**;11 doi 10.3389/fimmu.2020.583084.
80. Fridlender ZG, Buchlis G, Kapoor V, Cheng G, Sun J, Singhal S*, et al.* CCL2 blockade augments cancer immunotherapy. Cancer Res **2010**;70(1):109-18 doi 10.1158/0008-5472.Can-09-2326.
81. Zhang Y, Lazarus J, Steele NG, Yan W, Lee H-J, Nwosu ZC*, et al.* Regulatory T-cell Depletion Alters the Tumor Microenvironment and Accelerates Pancreatic Carcinogenesis. Cancer Discovery **2020**;10(3):422-39 doi 10.1158/2159-8290.Cd-19-0958.
82. Kim M, Choi HY, Woo JW, Chung YR, Park SY. Role of CXCL10 in the progression of in situ to invasive carcinoma of the breast. Scientific Reports **2021**;11(1):18007 doi 10.1038/s41598-021-97390-5.

83. Mao Z, Zhang J, Shi Y, Li W, Shi H, Ji R, *et al.* CXCL5 promotes gastric cancer metastasis by inducing epithelial-mesenchymal transition and activating neutrophils. Oncogenesis **2020**;9(7):63 doi 10.1038/s41389-020-00249-z.
84. Kessenbrock K, Plaks V, Werb Z. Matrix metalloproteinases: regulators of the tumor microenvironment. Cell **2010**;141(1):52-67 doi 10.1016/j.cell.2010.03.015.
85. Bhattacharya A, Chowdhury A, Chaudhury K, Shukla PC. Proprotein convertase subtilisin/kexin type 9 (PCSK9): A potential multifaceted player in cancer. Biochim Biophys Acta Rev Cancer **2021**;1876(1):188581 doi 10.1016/j.bbcan.2021.188581.
86. Qiao T, Yang W, He X, Song P, Chen X, Liu R, *et al.* Dynamic differentiation of F4/80+ tumor-associated macrophage and its role in tumor vascularization in a syngeneic mouse model of colorectal liver metastasis. Cell Death Dis **2023**;14(2):117 doi 10.1038/s41419-023-05626-1.
87. Tuit S, Salvagno C, Kapellos TS, Hau CS, Seep L, Oestreich M, *et al.* Transcriptional Signature Derived from Murine Tumor-Associated Macrophages Correlates with Poor Outcome in Breast Cancer Patients. Cell Rep **2019**;29(5):1221-35.e5 doi 10.1016/j.celrep.2019.09.067.
88. Guasconi L, Serradell MC, Garro AP, Iacobelli L, Masih DT. C-type lectins on macrophages participate in the immunomodulatory response to Fasciola hepatica products. Immunology **2011**;133(3):386-96 doi 10.1111/j.1365-2567.2011.03449.x.
89. Monteiro L, Pereira JAdS, Palhinha L, Moraes-Vieira PMM. Leptin in the regulation of the immunometabolism of adipose tissue-macrophages. Journal of Leukocyte Biology **2019**;106(3):703-16 doi https://doi.org/10.1002/JLB.MR1218-478R.
90. Linehan SA, Martínez-Pomares L, Stahl PD, Gordon S. Mannose receptor and its putative ligands in normal murine lymphoid and nonlymphoid organs: In situ expression of mannose receptor by selected macrophages, endothelial cells, perivascular microglia, and mesangial cells, but not dendritic cells. J Exp Med **1999**;189(12):1961-72 doi 10.1084/jem.189.12.1961.
91. Poon M-W, Jiang D, Qin P, Zhang Y, Qiu B, Chanda S, *et al.* Inhibition of NUCKS Facilitates Corneal Recovery Following Alkali Burn. Scientific Reports **2017**;7(1):41224 doi 10.1038/srep41224.
92. Liu T, Tan S, Xu Y, Meng F, Yang C, Lou G. Increased NUCKS expression is a risk factor for poor prognosis and recurrence in endometrial cancer. Am J Cancer Res **2015**;5(12):3659-67.
93. Drosos Y, Kouloukoussa M, Østvold AC, Grundt K, Goutas N, Vlachodimitropoulos D, *et al.* NUCKS overexpression in breast cancer. Cancer Cell Int **2009**;9:19 doi 10.1186/1475-2867-9-19.

94. Webster JD, Vucic D. The Balance of TNF Mediated Pathways Regulates Inflammatory Cell Death Signaling in Healthy and Diseased Tissues. Frontiers in Cell and Developmental Biology **2020**;8 doi 10.3389/fcell.2020.00365.

95. Mehta AK, Gracias DT, Croft M. TNF activity and T cells. Cytokine **2018**;101:14-8 doi 10.1016/j.cyto.2016.08.003.

96. Batlle E, Massagué J. Transforming Growth Factor-β Signaling in Immunity and Cancer. Immunity **2019**;50(4):924-40 doi 10.1016/j.immuni.2019.03.024.

97. Langlais D, Barreiro LB, Gros P. The macrophage IRF8/IRF1 regulome is required for protection against infections and is associated with chronic inflammation. J Exp Med **2016**;213(4):585-603 doi 10.1084/jem.20151764.

98. Mahmud SA, Manlove LS, Farrar MA. Interleukin-2 and STAT5 in regulatory T cell development and function. Jakstat **2013**;2(1):e23154 doi 10.4161/jkst.23154.

99. Mafi S, Mansoori B, Taeb S, Sadeghi H, Abbasi R, Cho WC*, et al.* mTOR-Mediated Regulation of Immune Responses in Cancer and Tumor Microenvironment. Front Immunol **2021**;12:774103 doi 10.3389/fimmu.2021.774103.

100. Yeh SCA, Hou J, Wu JW, Yu S, Zhang Y, Belfield KD*, et al.* Quantification of bone marrow interstitial pH and calcium concentration by intravital ratiometric imaging. Nature Communications **2022**;13(1):393 doi 10.1038/s41467-022-27973-x.

101. Yang K, Xu J, Fan M, Tu F, Wang X, Ha T*, et al.* Lactate Suppresses Macrophage Pro-Inflammatory Response to LPS Stimulation by Inhibition of YAP and NF-κB Activation via GPR81-Mediated Signaling. Front Immunol **2020**;11:587913 doi 10.3389/fimmu.2020.587913.

102. Stein M, Keshav S, Harris N, Gordon S. Interleukin 4 potently enhances murine macrophage mannose receptor activity: a marker of alternative immunologic macrophage activation. Journal of Experimental Medicine **1992**;176(1):287-92 doi 10.1084/jem.176.1.287.

103. Doherty TM, Kastelein R, Menon S, Andrade S, Coffman RL. Modulation of murine macrophage function by IL-13. The Journal of Immunology **1993**;151(12):7151-60 doi 10.4049/jimmunol.151.12.7151.

104. Doyle AG, Herbein G, Montaner LJ, Minty AJ, Caput D, Ferrara P*, et al.* Interleukin-13 alters the activation state of murine macrophages in vitro: Comparison with interleukin-4 and interferon-γ. European Journal of Immunology **1994**;24(6):1441-5 doi https://doi.org/10.1002/eji.1830240630.

105. Craver BM, El Alaoui K, Scherber RM, Fleischman AG. The Critical Role of Inflammation in the Pathogenesis and Progression of Myeloid Malignancies. Cancers (Basel) **2018**;10(4) doi 10.3390/cancers10040104.

106. Morrison BM, Tsingalia A, Vidensky S, Lee Y, Jin L, Farah MH*, et al.* Deficiency in monocarboxylate transporter 1 (MCT1) in mice delays regeneration of peripheral nerves following sciatic nerve crush. Exp Neurol **2015**;263:325-38 doi 10.1016/j.expneurol.2014.10.018.

107. Bisetto S, Whitaker-Menezes D, Wilski NA, Tuluc M, Curry J, Zhan T*, et al.* Monocarboxylate Transporter 4 (MCT4) Knockout Mice Have Attenuated 4NQO Induced Carcinogenesis; A Role for MCT4 in Driving Oral Squamous Cell Cancer. Front Oncol **2018**;8:324 doi 10.3389/fonc.2018.00324.

108. Bottomly D, Long N, Schultz AR, Kurtz SE, Tognon CE, Johnson K*, et al.* Integrative analysis of drug response and clinical outcome in acute myeloid leukemia. Cancer Cell **2022**;40(8):850-64.e9 doi https://doi.org/10.1016/j.ccell.2022.07.002.

109. Genomic and Epigenomic Landscapes of Adult De Novo Acute Myeloid Leukemia. New England Journal of Medicine **2013**;368(22):2059-74 doi 10.1056/NEJMoa1301689.

110. Pinho S, Lacombe J, Hanoun M, Mizoguchi T, Bruns I, Kunisaki Y*, et al.* PDGFRα and CD51 mark human nestin+ sphere-forming mesenchymal stem cells capable of hematopoietic progenitor cell expansion. J Exp Med **2013**;210(7):1351-67 doi 10.1084/jem.20122252.

111. Morikawa S, Mabuchi Y, Kubota Y, Nagai Y, Niibe K, Hiratsu E*, et al.* Prospective identification, isolation, and systemic transplantation of multipotent mesenchymal stem cells in murine bone marrow. J Exp Med **2009**;206(11):2483-96 doi 10.1084/jem.20091046.

112. Frisch BJ, Hoffman CM, Latchney SE, LaMere MW, Myers J, Ashton J*, et al.* Aged marrow macrophages expand platelet-biased hematopoietic stem cells via interleukin-1B. JCI Insight **2019**;4(10) doi 10.1172/jci.insight.124213.

113. Kriegler AB, Verschoor SM, Bernardo D, Bertoncello I. The relationship between different high proliferative potential colony-forming cells in mouse bone marrow. Experimental hematology **1994**;22(5):432-40.

114. Purton LE, Scadden DT. Limiting Factors in Murine Hematopoietic Stem Cell Assays. Cell Stem Cell **2007**;1(3):263-70 doi 10.1016/j.stem.2007.08.016.

115. Xu ZJ, Gu Y, Wang CZ, Jin Y, Wen XM, Ma JC*, et al.* The M2 macrophage marker CD206: a novel prognostic indicator for acute myeloid leukemia. Oncoimmunology **2020**;9(1):1683347 doi 10.1080/2162402x.2019.1683347.

116. Nordström F, Liegnell R, Apró W, Blackwood SJ, Katz A, Moberg M. The lactate receptor GPR81 is predominantly expressed in type II human skeletal muscle fibers: potential for lactate autocrine signaling. American Journal of Physiology-Cell Physiology **2023**;324(2):C477-C87 doi 10.1152/ajpcell.00443.2022.

117. Mayr B, Montminy M. Transcriptional regulation by the phosphorylation-dependent factor CREB. Nature Reviews Molecular Cell Biology **2001**;2(8):599-609 doi 10.1038/35085068.

118. Ruffell D, Mourkioti F, Gambardella A, Kirstetter P, Lopez RG, Rosenthal N*, et al.* A CREB-C/EBPβ cascade induces M2 macrophage-specific gene expression and promotes muscle injury repair. Proceedings of the National Academy of Sciences **2009**;106(41):17475-80 doi 10.1073/pnas.0908641106.

119. Jha Abhishek K, Huang Stanley C-C, Sergushichev A, Lampropoulou V, Ivanova Y, Loginicheva E*, et al.* Network Integration of Parallel Metabolic and Transcriptional Data Reveals Metabolic Modules that Regulate Macrophage Polarization. Immunity **2015**;42(3):419-30 doi https://doi.org/10.1016/j.immuni.2015.02.005.

120. Chen WL, Wang JH, Zhao AH, Xu X, Wang YH, Chen TL*, et al.* A distinct glucose metabolism signature of acute myeloid leukemia with prognostic value. Blood **2014**;124(10):1645-54 doi 10.1182/blood-2014-02-554204.

121. Wu G, Brosnan JT. Macrophages can convert citrulline into arginine. Biochemical Journal **1992**;281(1):45-8 doi 10.1042/bj2810045.

122. Hameed KM, Bollino DR, Shetty AC, Carter-Cooper B, Lapidus RG, Emadi A. Dual targeting of glutamine and serine metabolism in acute myeloid leukemia. Frontiers in Oncology **2024**;14 doi 10.3389/fonc.2024.1326754.

123. Chen J, Cui L, Lu S, Xu S. Amino acid metabolism in tumor biology and therapy. Cell Death & Disease **2024**;15(1):42 doi 10.1038/s41419-024-06435-w.

124. Angelin A, Gil-de-Gómez L, Dahiya S, Jiao J, Guo L, Levine MH*, et al.* Foxp3 Reprograms T Cell Metabolism to Function in Low-Glucose, High-Lactate Environments. Cell Metabolism **2017**;25(6):1282-93.e7 doi https://doi.org/10.1016/j.cmet.2016.12.018.

125. Szczepanski MJ, Szajnik M, Czystowska M, Mandapathil M, Strauss L, Welsh A*, et al.* Increased Frequency and Suppression by Regulatory T Cells in Patients with Acute Myelogenous Leukemia. Clinical Cancer Research **2009**;15(10):3325-32 doi 10.1158/1078-0432.CCR-08-3010.

126. Wang J, Huang H, Lu J, Bi P, Wang F, Liu X*, et al.* Tumor cells induced-M2 macrophage favors accumulation of Treg in nasopharyngeal carcinoma. Int J Clin Exp Pathol **2017**;10(8):8389-401.

127. Sun W, Wei F-Q, Li W-J, Wei J-W, Zhong H, Wen Y-H*, et al.* A positive-feedback loop between tumour infiltrating activated Treg cells and type 2-skewed macrophages is essential for progression of laryngeal squamous cell carcinoma. British Journal of Cancer **2017**;117(11):1631-43 doi 10.1038/bjc.2017.329.

128. Fujisaki J, Wu J, Carlson AL, Silberstein L, Putheti P, Larocca R*, et al.* In vivo imaging of Treg cells providing immune privilege to the haematopoietic stem-cell niche. Nature **2011**;474(7350):216-9 doi 10.1038/nature10160.

129. Chen Y, Feng Z, Kuang X, Zhao P, Chen B, Fang Q*, et al.* Increased lactate in AML blasts upregulates TOX expression, leading to exhaustion of CD8(+) cytolytic T cells. Am J Cancer Res **2021**;11(11):5726-42.

Tables attached as Excel Files (other tables can be found in Supplementary)

Table 1: Significantly Altered Extracellular Metabolites in Human AML Bone Marrow

Table 2: Cytokines Upregulated in LAM Cocultures and Reported Functions in the BM or Cancer Progression

Table 3: Differential Expression - Common Upregulated Elements in LAMs and TAMs

Table 4: Gene Set Enrichment Analysis – Hallmark Genes Enriched in LAMs as Compared to TAMs from Both Colorectal Metastasis and Breast Cancer

Figure Legends

Fig. 1) Lactate is elevated in the bone marrow microenvironment (BMME) during acute myeloid leukemia (AML).

A-C, Metabolomics of bone marrow serum from AML patients or normal controls: Graphical depiction of procedure (**A**), heatmap showing the relative abundance of detectable metabolites (**B**), and scores plot of principal component analysis (**C**) (n = 4, in triplicates). **D,** Lactate concentration in AML and normal bone marrow (BM) serum (n = 4). Significance level determined by unpaired t test for **B** and **D** are indicated as: *, $P < 0.05$; **, $P < 0.01$; ***, $P < 0.001$; ****, $P < 0.0001$. Error bar indicates mean ± standard deviation (SD).

Fig. 2) Lactate contributes to the polarization of leukemia-associated macrophage (LAMs) to an alternatively activated phenotype.

A, Gating scheme for flow cytometric analysis of polarization markers on murine macrophages. **B,** Simplified Presentation of Incredibly Complex Evaluations (SPICE) analysis of LAM subpopulations from late-stage bcCML (55-70% GFP^+ cells in BM) (n = 5), arrows indicate population enriched in disease. **C** and **D,** Frequency of $CD206^{hi}$ (**C**) and expression level by mean fluorescence intensity (MFI) of CD206 on $CD206^+$ (**D**) nonleukemic control macrophages (Ctrl), leukemia-associated macrophages (LAMs), or leukemic (GFP^+) macrophages (n = 7). **E** and **F,** Bulk RNA sequencing of LAMs vs. macrophages from nonleukemic (NL) controls: heatmap of differentially expressed genes (**E**) and principal component analysis (PCA) of the top 500 variable genes (**F**). **G,** Cytokine profiling of media from macrophages sorted from nonleukemic or leukemic mice and cultured for four days (n = 2), representative example, arrows indicate a qualitative difference. **H,** Venn diagrams displaying the number of GO pathways significantly upregulated or downregulated by $F4/80^+$ cancer-associated

macrophages compared to each study's own healthy controls: by bcCML LAMs (n = 6) or tumor-associated macrophages (TAM) from murine models of colorectal liver metastasis (CM) (n = 5) or breast cancer (BC) (n = 3). **I,** Hallmark gene sets enriched in LAMs compared directly to TAMs, as determined by gene set enrichment analysis (GSEA): Venn diagram displaying numbers of significantly enriched gene sets, and representative enrichment plots of top significant sets. Significance levels determined by one-way ANOVA for **C** and **D,** are indicated as: ***, $P < 0.001$; ****, $P < 0.0001$. Error bar indicates mean ± SD. Significance for **I** was determined by GSEA as an FDR q-value of < 0.25.

Fig. 3) Lactate-GPR81 signaling contributes to leukemia-associated macrophage (LAM) polarization.

A and **B,** Expression level of CD206 on bone marrow-derived macrophages polarized *in vitro* by treatment with 10 mmol/L lactate, lipopolysaccharide (LPS) as proinflammatory stimuli, and/or IL-4 and IL-13 as suppressive stimuli, in serum-free media for 12 hours (**A**) (n = 6) or 1 week (**B**) (n = 3). **C,** Following polarization with 10 mmol/L of lactate and 5 ng/mL of IL-4 and IL-13 (ILs), fold change of CD206 expression on $CD206^{+}$ BMDMs 48 hours after removal of stimuli by media change relative to untreated control (n = 2-4). **D,** Graphical depiction of the initiation of wt bcCML in a *Gpr81*$^{-/-}$ BMME. **E-H,** Flow cytometric analysis of live nonleukemic (GFP^{-}) bone marrow cells from wt bcCML initiated in wt or *Gpr81*$^{-/-}$ (GPR81KO) mice or nonleukemic (NL) controls: fold change frequency of macrophages relative to NL controls of the same genetic background (**E**) (n = 4-7), frequency of $CD206^{+}$ macrophages (**F**), expression level of CD206 on $CD206^{+}$ BM macrophages relative to NL controls of the same genetic background (**G**), frequency of $MHCII^{+}$ BM macrophages (**H**) (n = 4-11). **I,** MFI of CD206 on $CD206^{+}$ wt or *Gpr81*$^{-/-}$ BMDMs treated with LPS, ILs, and/or 10 mmol/L lactate (n = 3). **J,** Frequency of $CD206^{hi}$ wt or $GPR81^{-/-}$ BMDMs with or without polarization by ILs and lactate.

Significance levels determined by one-way ANOVA for **A-B, E-H,** and **I-J** are indicated as: ns, not significant; *, $P < 0.05$; **, $P < 0.01$; ***, $P < 0.001$; ****, $P < 0.0001$. Error bar indicates mean ± SD.

Fig. 4) GPR81 signaling on leukemic cells drives expansion rate and leukemia stem cell (LSC) self-renewal.

A, Graphical depiction of the production of *Gpr81*$^{-/-}$ (GPR81KO) bcCML cells and initiation in GPR81KO mice (GPR81 DKO). **B-D,** Leukemic burden in the bone marrow (BM) (**B**), peripheral blood (**C**), and spleen (**D**), of wt or GPR81KO bcCML by the timepoint of wt late-stage disease (n = 5). **E,** Leukemic burden in the BM over time of wt or GPR81KO bcCML (n = 5-7). **F,** Time to progression to late-stage disease in wt or GPR81 DKO bcCML (n = 5). **G** and **H,** LSC repopulation assays of wt vs. *Gpr81*$^{-/-}$ bcCML cells: number of colonies at each passage (**G**)**,** and probability of survival by passage (**H**) (n = 3, in duplicates). Significance levels determined by unpaired t tests for **B-E**, and log-rank (Mantel-Cox) test for **F** and **H**, are indicated as: *, $P < 0.05$; **, $P < 0.01$; ***, $P < 0.001$. Error bar indicates mean ± SD.

Fig. 5) Lactate drives loss of hematopoietic stem and progenitor cell (HSPC) function and support.

A, Fold change colony-forming unit cell (CFU-C) colonies of HSPCs with or without lactate treatment for 72 hours, relative to the 0 mmol/L lactate control group (n = 7-10). **B** and **C,** HSPCs cocultured on a bone marrow (BM) stromal monolayer for 72 hours with or without lactate treatment: graphic of experimental procedure (**B**) and fold change CFU-Cs relative to the 0 mmol/L lactate control group (**C**) (n = 12-14). **D** and **E,** HSPCs cocultured with a BM stromal monolayer and either 60,000 added LAMs or healthy control (Ctrl) macrophages for four days: graphical depiction of procedure (**D**) and fold change CFU-Cs relative to control group (**E**) (n = 4). **F-H,** Relative area of colony forming units (CFU) of BM mesenchymal stem cells with or without lactate treatment past day 4: after 14 days differentiation to pre-osteoblastic (CFU-preOB) colonies (**F**) (n = 6), fibroblastic colonies (CFU-F) after

10 days culture in non-differentiation media (**G**) (n = 6), and representative images (**H**). Significance levels determined by one-way ANOVA for **A**, **C**, **F**, and **G**, or by unpaired t test for **E** are indicated as: ***, $P < 0.001$; ****, $P < 0.0001$. Error bar indicates mean ± SD.

Fig. 6) GPR81 signaling partially regulates HSPC function and does not impact critical bone marrow hematopoietic support.

A-F, Wt bcCML initiated in wt or GPR81KO mice, hematopoietic progenitors' frequency in the bone marrow relative to the nonleukemic (NL) control of the same genetic background: hematopoietic stem and progenitor cells (HSPCs/LSK) (**A**), long-term hematopoietic stem cell (HSC) (**B**), short-term HSC (**C**), multipotent progenitor (MPP) subsets MPP2 (**D**) MPP3 (**E**) and MPP4 (**F**) (n = 4). **G** and **H,** CFU-Cs of wt or *Gpr81*$^{-/-}$ (G) lactate-treated HSPCs cultured alone (**G**) (n = 4-13) or cocultured with a stromal monolayer (**H**) (n = 3-7), relative to the 0 mmol/L lactate control group of the same genetic background. **I** and **J,** CFU-preOB (**I**) and CFU-F (**J**) of wt or *Gpr81*$^{-/-}$ MSCs with lactate treatment, relative to the 0 mmol/L lactate control of the same genetic background. Significance levels determined by one-way ANOVA for all are indicated as: ns, not significant; *, $P < 0.05$; **, $P < 0.01$; ***, $P < 0.001$; ****, $P < 0.0001$. Error bar indicates mean ± SD.

Fig. 1)

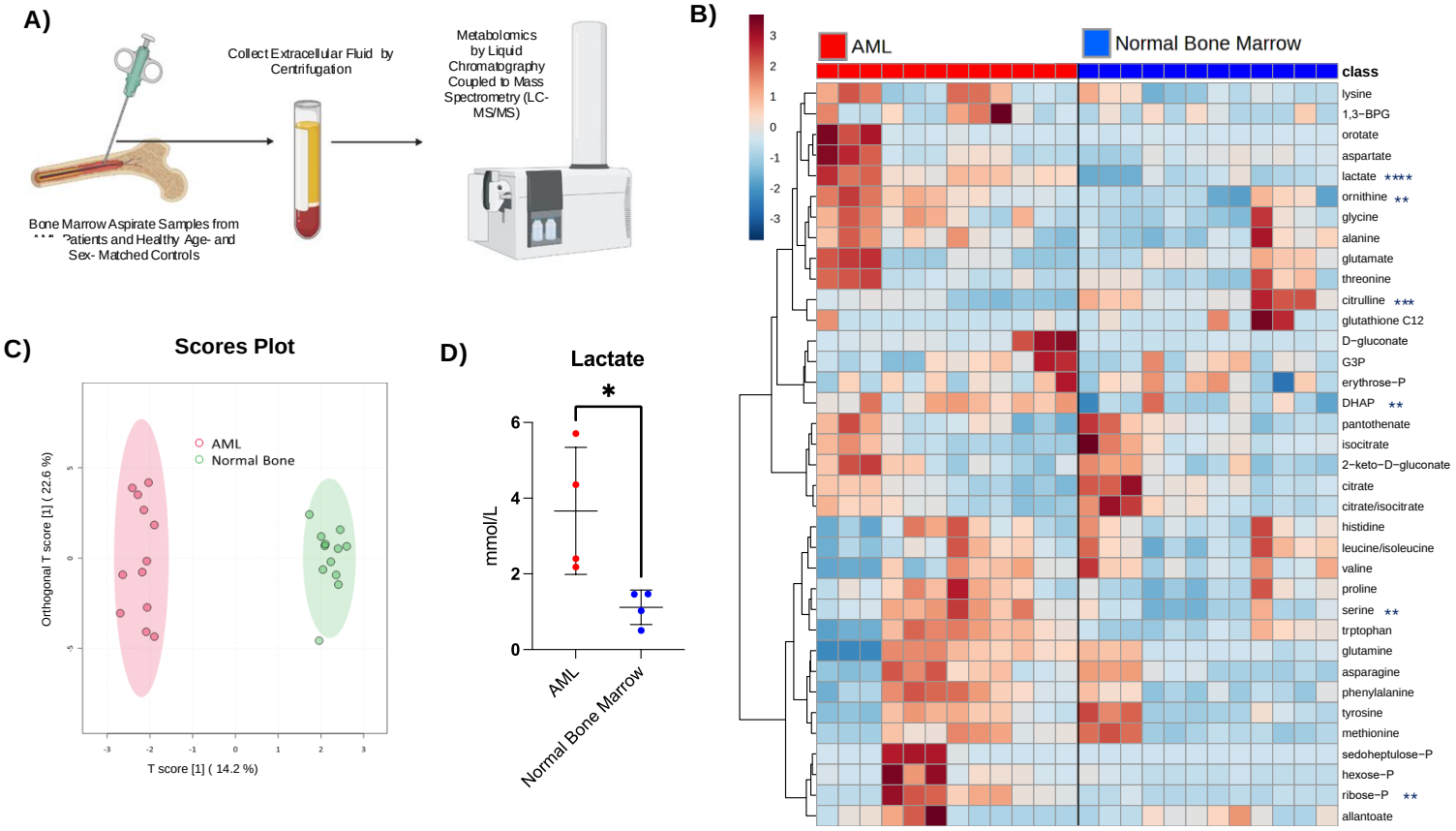
A)
Collect Extracellular Fluid by Centrifugation
Metabolomics by Liquid Chromatography Coupled to Mass Spectrometry (LC-MS/MS)
Bone Marrow Aspirate Samples from AML Patients and Healthy Age- and Sex- Matched Controls
B)
AML
Normal Bone Marrow
class
lysine
1,3−BPG
orotate
aspartate
lactate ****
ornithine **
glycine
alanine
glutamate
threonine
citrulline ***
glutathione C12
D−gluconate
G3P
erythrose−P
DHAP **
pantothenate
isocitrate
2−keto−D−gluconate
citrate
citrate/isocitrate
histidine
leucine/isoleucine
valine
proline
serine **
trptophan
glutamine
asparagine
phenylalanine
tyrosine
methionine
sedoheptulose−P
hexose−P
ribose−P **
allantoate
C)
Scores Plot
AML
Normal Bone
Orthogonal T score [1] (22.6 %)
T score [1] (14.2 %)
D)
Lactate
*
mmol/L
AML
Normal Bone Marrow

Fig. 2)

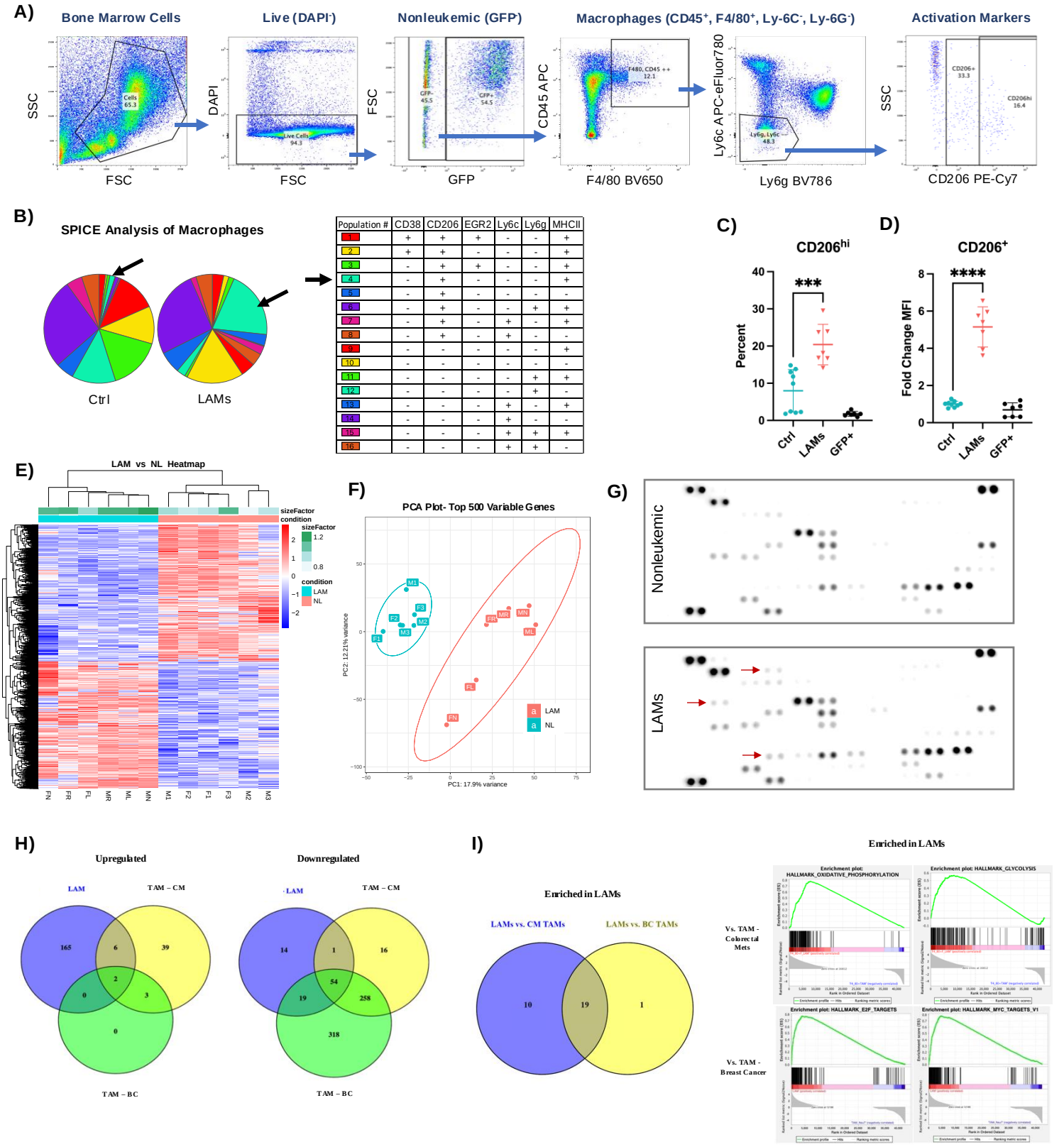

Population #	CD38	CD206	EGR2	Ly6c	Ly6g	MHCII
1	+	+	+	-	-	+
2	+	+	-	-	-	+
3	-	+	+	-	-	+
4	-	+	-	-	-	+
5	-	+	-	-	-	-
6	-	+	-	-	+	+
7	-	+	-	+	-	+
8	-	+	-	+	-	-
9	-	-	-	-	-	+
10	-	-	-	-	-	-
11	-	-	-	-	+	+
12	-	-	-	-	+	-
13	-	-	-	+	-	+
14	-	-	-	+	-	-
15	-	-	-	+	+	+
16	-	-	-	+	+	-

Fig. 3)

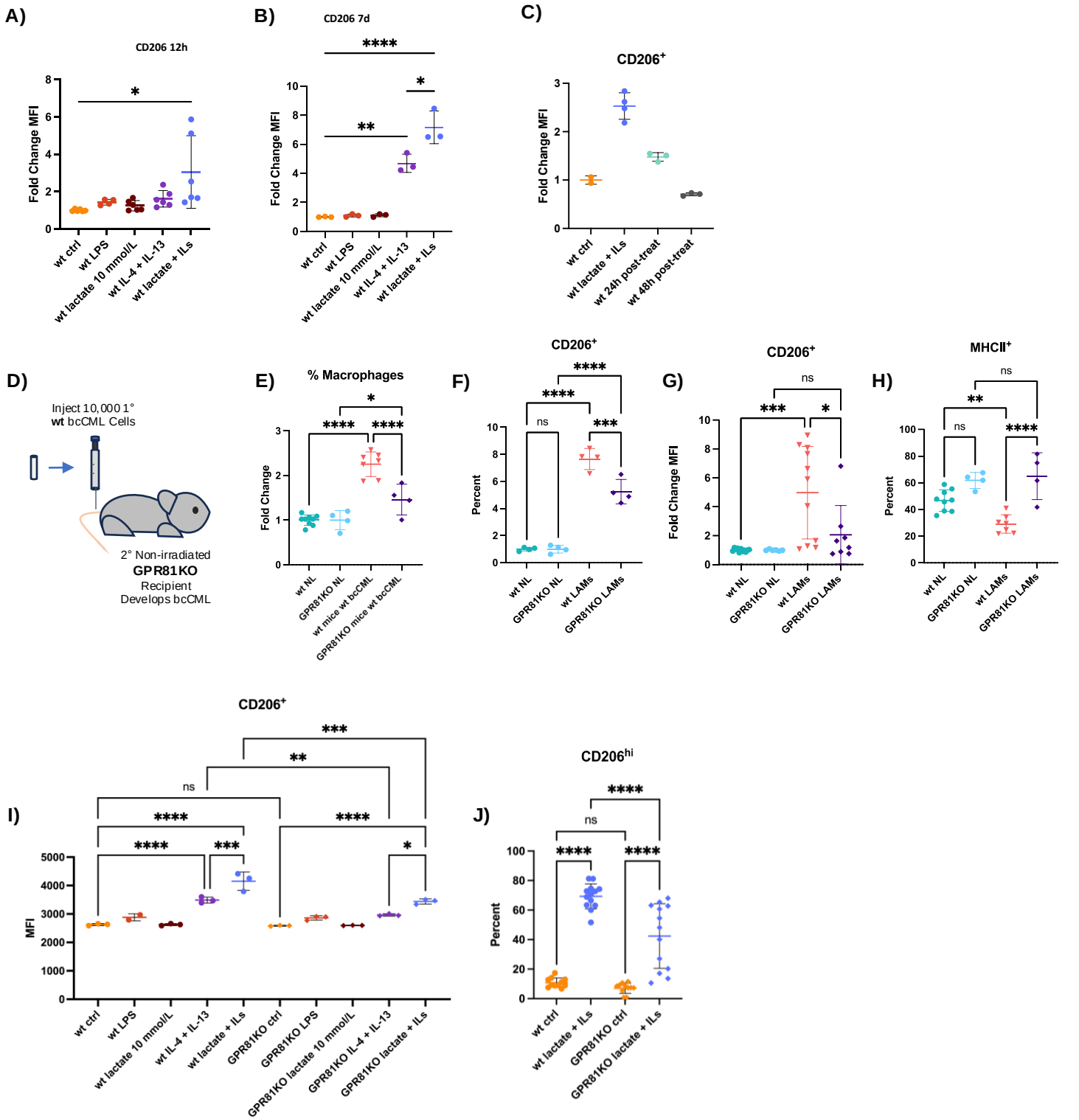
A)
CD206 12h
Fold Change MFI
wt ctrl
wt LPS
wt lactate 10 mmol/L
wt IL-4 + IL-13
wt lactate + ILs
B)
CD206 7d
Fold Change MFI
C)
CD206+
Fold Change MFI
wt 24h post-treat
wt 48h post-treat
D)
Inject 10,000 1° wt bcCML Cells
2° Non-irradiated GPR81KO Recipient Develops bcCML
E)
% Macrophages
Fold Change
wt NL
GPR81KO NL
wt mice wt bcCML
GPR81KO mice wt bcCML
F)
CD206+
Percent
wt LAMs
GPR81KO LAMs
G)
CD206+
Fold Change MFI
H)
MHCII+
Percent
I)
CD206+
MFI
GPR81KO ctrl
GPR81KO LPS
GPR81KO lactate 10 mmol/L
GPR81KO IL-4 + IL-13
GPR81KO lactate + ILs
J)
CD206hi
Percent

Fig. 4)

A)

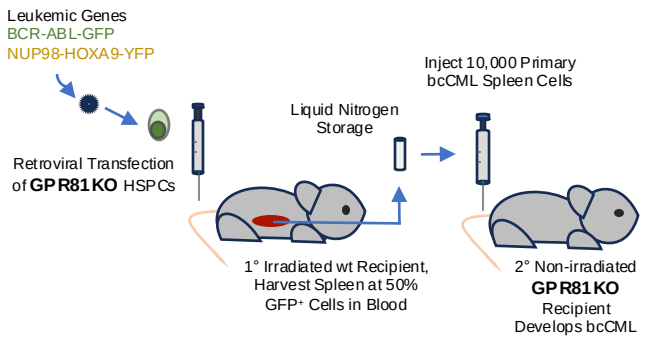

B)

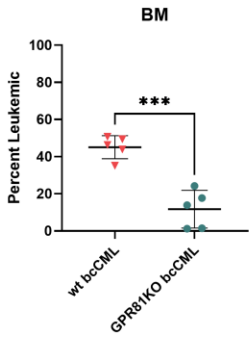

C)

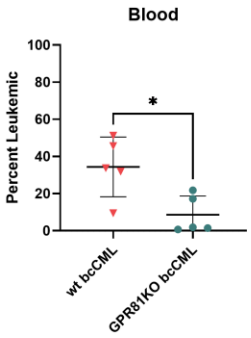

D)

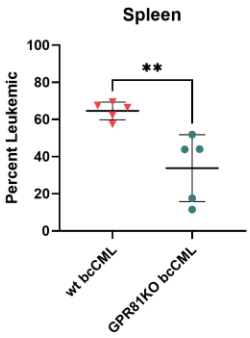

E)

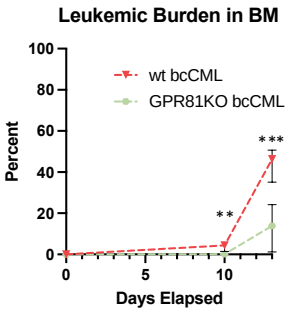

F)

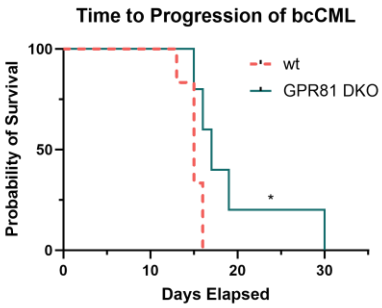

G)

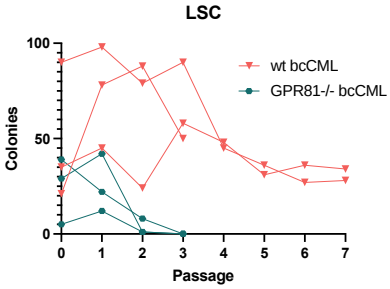

H)

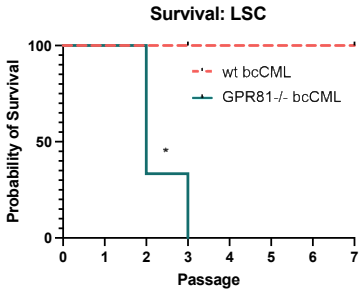

Fig. 5)

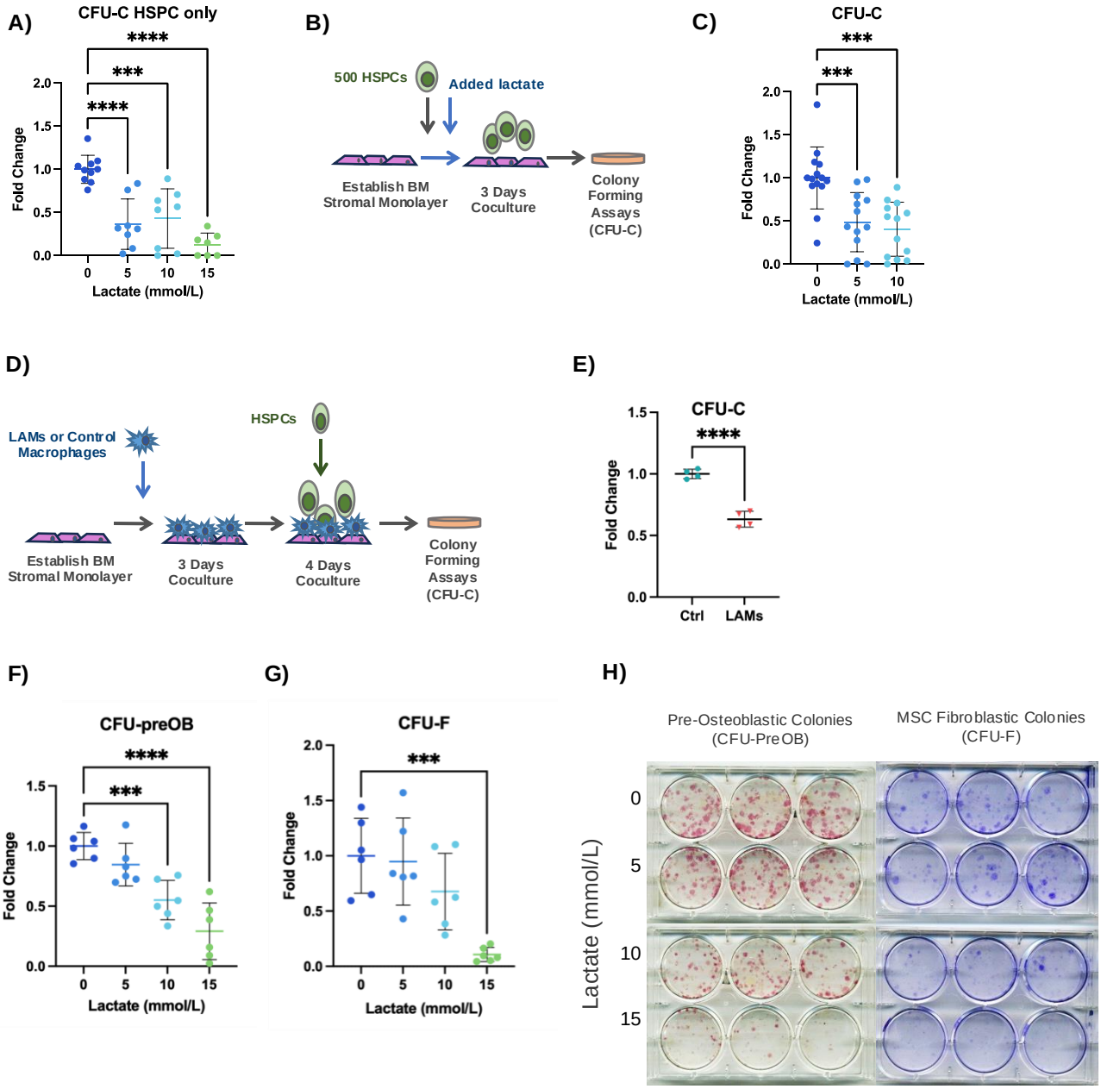
A)
CFU-C HSPC only
****
***
****
Fold Change
2.0
1.5
1.0
0.5
0.0
0
5
10
15
Lactate (mmol/L)
B)
500 HSPCs
Added lactate
Establish BM Stromal Monolayer
3 Days Coculture
Colony Forming Assays (CFU-C)
C)
CFU-C
***
***
Fold Change
2.0
1.5
1.0
0.5
0.0
0
5
10
Lactate (mmol/L)
D)
LAMs or Control Macrophages
HSPCs
Establish BM Stromal Monolayer
3 Days Coculture
4 Days Coculture
Colony Forming Assays (CFU-C)
E)
CFU-C
****
Fold Change
1.5
1.0
0.5
0.0
Ctrl
LAMs
F)
CFU-preOB
****
***
Fold Change
1.5
1.0
0.5
0.0
0
5
10
15
Lactate (mmol/L)
G)
CFU-F
***
Fold Change
2.0
1.5
1.0
0.5
0.0
0
5
10
15
Lactate (mmol/L)
H)
Pre-Osteoblastic Colonies (CFU-PreOB)
MSC Fibroblastic Colonies (CFU-F)
Lactate (mmol/L)
0
5
10
15

Fig. 6)

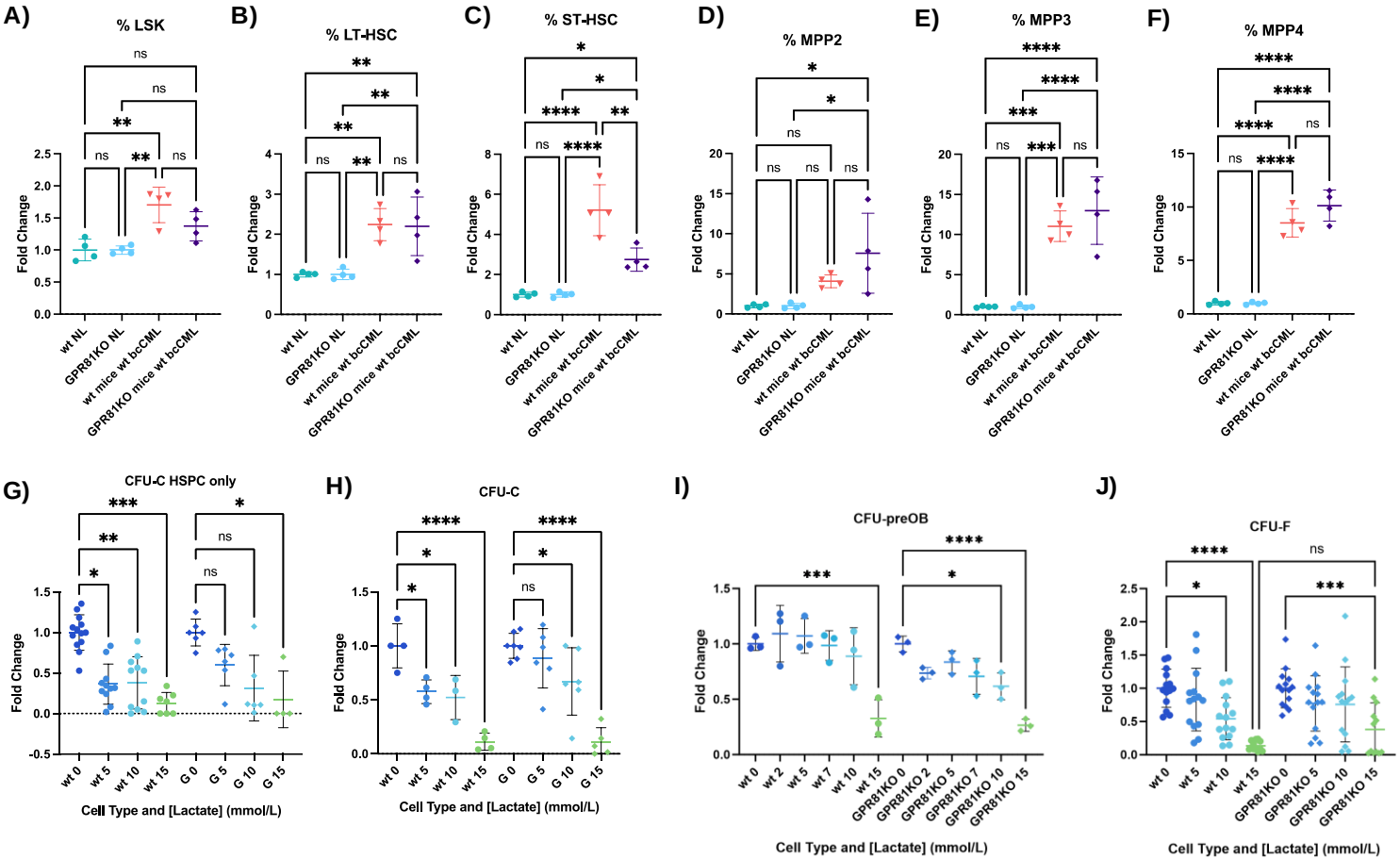
A)
% LSK
B)
% LT-HSC
C)
% ST-HSC
D)
% MPP2
E)
% MPP3
F)
% MPP4
Fold Change
wt NL
GPR81KO NL
wt mice wt bcCML
GPR81KO mice wt bcCML
G)
CFU-C HSPC only
H)
CFU-C
I)
CFU-preOB
J)
CFU-F
Cell Type and [Lactate] (mmol/L)

Compound	t Stat	p Value	-log10(p)	FDR
lactate	5.8818	6.42E-06	5.1922	0.000224
citrulline	-4.0561	0.00052604	3.279	0.0092
serine	3.748	0.0011128	2.9536	0.00974
DHAP	3.6597	0.0013779	2.8608	0.00974
ribose-P	3.6554	0.0013923	2.8563	0.00974
ornithine	3.4174	0.0024667	2.6079	0.0143

Table 1: Significantly Altered Extracellular Metabolites in Human AML Bone Marrow

Cytokine	Reported Functions
CXCL10/IP-10	Immunosuppressive Tumor Microenvironment
CCL12 (MCP-5)	Immunosuppressive Tumor Microenvironment
CCL6/C10 (MRP-1)	Immunosuppressive Tumor Microenvironment
Proprotein Convertase 9 (PCSK9)	Tumor Growth and Metastasis, and Immunosuppressive Tumor Microenvironment
LIX (CXCL5)	Tumor Growth and Metastasis
MMP3	Tumor Growth and Metastasis

Table 2: Cytokines Upregulated in LAM Cocultures and Reported Functions in the BM or Cancer Progression

2 Common Upregulated Elements in LAMs and Both Types of TAMs	6 Common Upregulated Elements in LAMs and Colorectal Mets TAMs	3 Common Upregulated Elements in Colorectal Mets TAMs and Breast Cancer TAMs
C-type lectin receptor (CLR) signaling pathway	Apoptosis	Lysosome
NUCKS1 24931609 ChIP-Seq HEPATOCYTES Mouse	Toxoplasmosis	TYROBP Causal Network WP3625
	Chagas disease (American trypanosomiasis)	Microglia Pathogen Phagocytosis Pathway WP3626
	TNF signaling pathway	
	IRF8 27001747 Chip-Seq BMDM Mouse	
	TGF Beta Signaling Pathway WP113	

Table 3: Differential Expression - Common Upregulated Elements in LAMs and TAMs

Gene sets Enriched in LAM vs. both Colorectal Mets TAMs and Breast Cancer TAMs
HALLMARK_E2F_TARGETS
HALLMARK_OXIDATIVE_PHOSPHORYLATION
HALLMARK_MYC_TARGETS_V1
HALLMARK_DNA_REPAIR
HALLMARK_MYC_TARGETS_V2
HALLMARK_MTORC1_SIGNALING
HALLMARK_G2M_CHECKPOINT
HALLMARK_HEME_METABOLISM
HALLMARK_UNFOLDED_PROTEIN_RESPONSE
HALLMARK_FATTY_ACID_METABOLISM
HALLMARK_ADIPOGENESIS
HALLMARK_REACTIVE_OXIGEN_SPECIES_PATHWAY
HALLMARK_PEROXISOME
HALLMARK_GLYCOLYSIS
HALLMARK_ALLOGRAFT_REJECTION
HALLMARK_SPERMATOGENESIS
HALLMARK_ESTROGEN_RESPONSE_LATE
HALLMARK_BILE_ACID_METABOLISM
HALLMARK_XENOBIOTIC_METABOLISM

Table 4: Gene Set Enrichment Analysis – Hallmark Genes Enriched in LAMs as Compared to TAMs from Both Colorectal Metastasis and Breast Cancer